G.A.308469

Collaborative Project of the 7th Framework Programme

Work Package 8

GIS analysis and data-layers integration

D8.6: Report of early findings regarding congruence between crowd-sourced, external and calibrated data

Version 2.0

09/02/2015

www.Citclops.eu

Document Information

Project Number	308469	**Acronym**	Citclops
Full title	Citizens' observatory for coast and ocean optical monitoring		
Project URL	http://www.Citclops.eu		
EU Project officer	Gilles Ollier		

Deliverable	**Number**	8.6	**Title**	Report of early findings regarding congruence between crowd-sourced, external and calibrated data
Work package	**Number**	8	**Title**	GIS analysis and data-layers integration

Date of delivery	**Contractual**	PM24	**Actual**	PM29
Status			final ☑	
Nature	Prototype ☐ Report ☑ Dissemination ☐ Other ☐			
Dissemination Level	Public (PU) ☑ Restricted to other programme participants (PP) ☐ Restricted to a group specified by the consortium (RE) ☐ Consortium (CO) ☐			

Authors (Partner)	H.J. van der Woerd (VU-VUmc) with major contributions from CSIC, NIOZ, UNIOL, NOVELTIS			
Responsible Author	H.J, van der Woerd		**Email**	Hans.van.der.woerd@ivm.vu.nl
	Partner	VU-VUmc	**Phone**	+31 20 598 9565

Abstract (for dissemination)	This is a report on the early findings, regarding the congruence between crowd-sourced, external and calibrated data. It is based on material that has been collected in field campaigns in 2011 and 2013. Colour measurement were analysed from the liquid and plastic FU scale, RAMSES spectrometers above and below water, Samsung S3 images and MERIS scenes. Light attenuation was measured with the Citclops low-cost KdUINO instrument and the high-cost PRR-800 High Resolution Profiling Reflectance Radiometer. These measurements were correlated for a first ever characterisation of bias and noise of these citizen tools.
Keywords	Data analysis, bias, chromaticity, MERIS, Ebro Delta, KdUINO

Version Log			
Issue Date	**Version**	**Author**	**Change**
10/01/2015	1.0	Hans van der Woerd	Version 1.0
19/01/2015	1.1	Hans van der Woerd	Check by dr. J. Busch (UNIOL)
04/02/2015	1.2	Luigi Ceccaroni	Scientific-coordinator review
09/02/2015	2.0	Jesús Fernández	Format review

Table of contents

List of Figures

List of tables

1 Introduction

An important aspect of using citizen science to collect environmental data is quality control. The data are coming from various sources and are collected under different conditions, which will influence the quality of the observations and their use. For wider use it is required to validate these observations by means of data quality control procedures and a tie-in with independent satellite-based and ground-based observations.

In this document we report on the first outcome of multiple experiments that were aimed to the characterisation of bias and standard errors of low-cost sensors and information from the Citclops App. We report on these to show progress and draw first conclusions on the congruence of data and identify points that need closer inspection.

The four chapters are based on presentations to the scientific community at conferences and in publications. It is important for decision makers and the public that the methods used in Citclops are known and scrutinized by the scientific community. In order to archive these contributions and report to the EC in a public deliverable, three out of four contributions are integral copies of the conference proceedings. The fourth is based on the manuscript that is submitted to a high-impact journal (Science of the Total Environment, Elsevier).

1.1 Reference documents

Chapter 2:
Busch, J.A., Bernard, E. Jeansou, E. Price, I., Van der Woerd, H., Zielinski, O., 2014. Changes of water colour in the aquaculture zone of the Ebro Delta, NW Mediterranean - pilot site for citizen observatory. Presented at the Ocean Optics Conference XXII 26-31 October 2014, Portland, USA.

Chapter 3:
Novoa, S., Wernand, M., Van der Woerd, H.J. 2014. The Forel-Ule scale converted to modern tools for participatory water quality monitoring. Presented at the Ocean Optics Conference XXII 26-31 October 2014, Portland, USA.

Chapter 4:
Novoa, S., Wernand, M., Van der Woerd, H.J., 2015. WACODI: A generic algorithm to derive the intrinsic colour of natural waters from digital images. Science of the Total Environment. Submitted Manuscript.

Chapter 5:
R. Bardají, Zafra, E., Simon, C., and Piera, J., 2014. Comparing water transparency measurements obtained with low-cost citizens science instruments and high-quality oceanographic instruments. OCEANS'14 MTS/IEEE 7-11 April, Taipei, Taiwan.

2 The Ebro delta case study

2.1 SUMMARY

Changes in water colour are linked to a number of processes of concern to society, including algal blooms. In order to motivate citizens to get engaged in environmental monitoring and to improve their environmental science capacity, bio-optical measurement tools for citizens are developed within the EU project "Citclops" (Citizens' observatory for Coast and Ocean Optical Monitoring). Key parameter is an assessment of water colour by comparison to the Forel Ule (FU) colour scale. In one of the two Citclops test areas, the Ebro Delta, NW Mediterranean, measurements of water colour with the FU scale along weekly transects from May – June 2011 revealed colour changes over short distances and time frames, indicative of fast dynamics of phytoplankton in the area. The typical seasonal pattern of phytoplankton proliferations was reflected well by FU colours as retrieved from satellite data (Medium Resolution Imaging Spectrometer (MERIS) full resolution 300m data). The results show that a simplified classification of natural waters by its colour enhances our understanding of spatio-temporal dynamics in the Ebro Delta. Hence, such measurements can complement more accurate in-situ observations that allow the identification of harmful algal taxa and phycotoxins. Thereby, Citclops observations support phytoplankton surveillance for human health and food safety. Direct links to environmental issues strongly motivate the general public to engage in environmental surveillance and stewardship, and to support local monitoring efforts.

2.2 INTRODUCTION

Changes in water colour are directly linked to alterations in water composition, in particular phytoplankton biomass and community assembly. These relate to a number of processes of concern to society like algal blooms. In order to measure these parameters, and improve the environmental science capacity of citizens, the importance of their active involvement is gaining increased recognition. The impact of public participation in the best case leads to a conservation of the environment by forming knowledge and identity of individuals, providing a basis for relationships and legislation of social-ecological systems and scientific data to answer scientific questions as overlapping outcomes, see Figure 1 (*1*).

Within the EU project Citclops both aspects are addressed. The overall aim is to equip citizens with tools by transfer of bio-optical measurements to smartphone apps, and to improve their general knowledge of the environment. In order to motivate citizens and enable their participation, they need to know what, how, and why to measure. On the project website (www.citclops.eu) and in dedicated citizen training events, fundamental bio-optical principles and the resulting relation of water colour to constituents, such as phytoplankton, suspended solids and coloured dissolved organic material (CDOM) is transferred to the public, e.g. with a colour wheel (Figure 2). Water colour measurement in Citclops is simplified to a comparison with 21 colours (blue to brown) on the Forel Ule (FU) colour scale (compare *2*). The assignment of colours by citizens is performed either with a plastic scale above water, or by a digital scale above a photo in the Citclops smart phone app. Information on how to measure are provided on website and directly in the app. In development are a quality control procedure for images (*3*) and a seasonal fit with background images of typical regional FU colours for the two Citclops core regions Wadden Sea and Ebro Delta. For this purpose, a data extraction service for MERIS full resolution satellite data has been developed, based on version 2 of the DUE Coastcolour project (www. coastcolour.org).

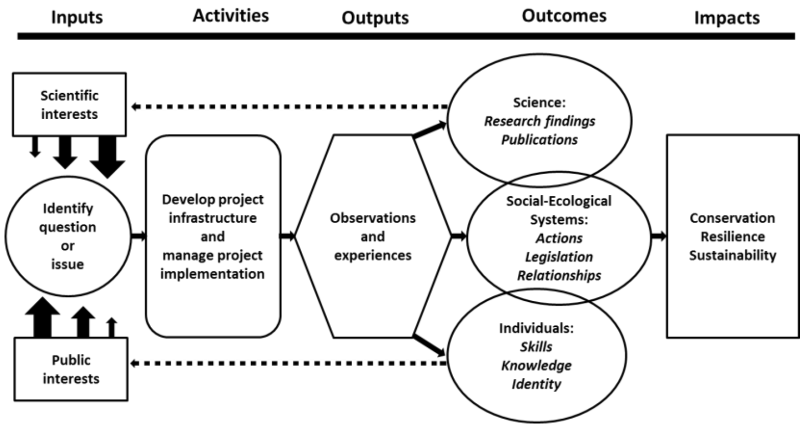

Figure 1 Scheme of public participation in scientific research project, including feedback arrows. Balanced input from scientific and public interest, negotiated differently by each project are visualised, as well as different overlapping outcomes for science, social-ecological systems and individuals (Use of figure courtesy J. Shirk)

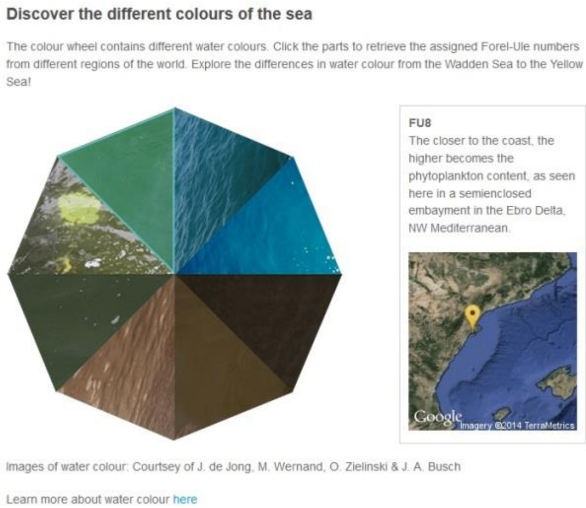

Figure 2 Citclops colour wheel for citizen´s education: Different water colours from around the world are assigned to corresponding Forel Ule values. A change of colour and FU numeral equals a change of water constituents. Source: http://citclops.eu/education/colour-wheel--water-colours-explained

The Ebro Delta is a touristic area and is known for seafood, fisheries and leisure activities in two semi-enclosed embayments: Alfacs and Fangar (Figure 3). Hydrodynamics in both bays are influenced by the surrounding Mediterranean Sea and seasonally by freshwater inflow through channels from an irrigation system for rice agriculture. Such changes in water regimes can influence the presence of algal species including taxa which are capable to produce potent phycotoxins. This is by simple transport of algal blooms from the Mediterranean, provision of good conditions for already present species in the bay´s zones with long retention times (*4*), or by providing favourable environmental conditions, e.g. by nutrient inflow from terrestrial activities via irrigation canals (*5*). Typically, algal biomass (by proxy of the algal pigment chlorophyll *a* (Chl *a*)) follows a pattern of increase towards end of summer/autumn in both embayments, with earlier start in Fangar Bay (*6*). Three major potentially noxious algal genera are known for high biomass production in the bays: dinoflagellate *Karlodinium* spp., diatom *Pseudo-nitzschia* spp. (*7-8*) and occasionally the raphidophyte *Chattonella* spp. (M. Fernández-Tejedor, pers. comm.).

In this study we present the first results of a direct comparison of in-situ and satellite colour data in both Alfacs and Fangar bay for the year 2011 in order to test compatibility, strengths and weaknesses of both methods and the information shown by colour monitoring.

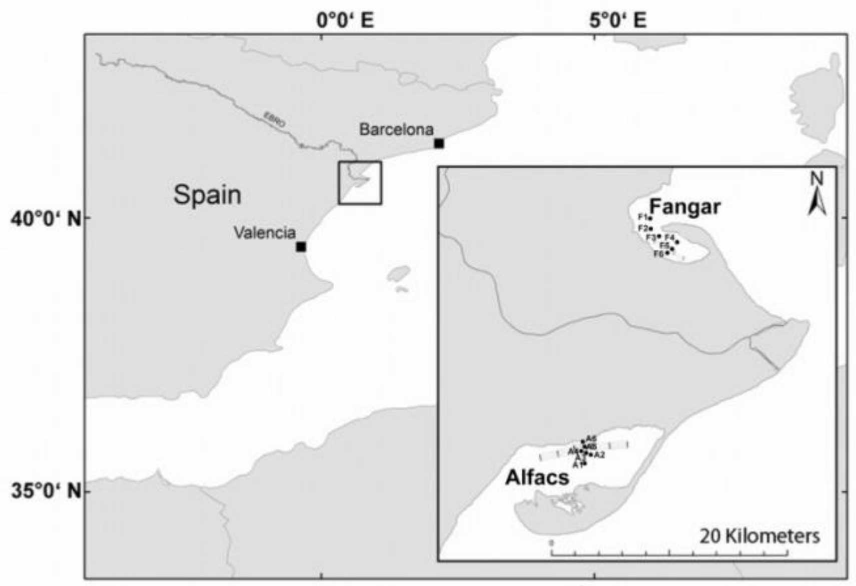

Figure 3 The two semi-enclosed embayments Alfacs Bay and Fangar Bay are in the Ebro Delta natural park on the NW Mediterranean coast. Forel Ule (FU) water colour was measured and modelled at six stations in both bays (dots), A1-A6 in Alfacs Bay, F1-F6 in Fangar Bay, including positions at the centre of the bays and close to the aquaculture facilities (black pattern).

2.3 METHODS

Water colour was measured at six stations along transects during nine cruises in Alfacs Bay and five cruises in Fangar Bay, in May and June 2011 (Figure 3). Water colour above a submerged white Secchi disk at half Secchi depth was assigned colour standards of a LaMotte colour scale (LaMOTTE COMPANY, Maryland, USA) and assigned to the matching FU numeral (1-21). Corresponding to FU measurements at station A4 in Alfacs Bay, remote sensing reflectance spectra were collected from a set of three Ramses spectrometers that measured the water-leaving radiance, matching sky radiance and downward irradiation (*9*). These were assigned to FU numbers by means of conversion to chromaticity coordinates and matched to FU coordinates following Wernand *et al*. (*10*) and Novoa *et al*. (*2*).

MERIS scenes of the Ebro Delta area for the year 2011 were downloaded from the coastcolour ftp site, extracted and projected on a standard lat-lon grid. Based on the L2R products, the information of band 1-9 (412-708 nm) was converted to FU values by means of the FUME algorithm (*10*). At the position of all 12 ground stations, the nearest nine pixels were selected to test the variability in information near the stations and give some means for data quality control. The MERIS overpass is always in the morning (between 9:53 and 10:53 UTC) and 142 scenes are available in 2011. From the available pixels (142 times 9) at station A4 near 45% contained no data due to clouds or failure in the processing to L2R products. Only in 24% of the cases all 9 pixels contained reliable data.

2.4 RESULTS

Water colour as measured with the LaMotte scale, as well as derived by reflectance data from the A4 platform station and MERIS ranged from blue-green to brownish green during the respective study time. Measured FU values are in quite similar for the Alfacs station, but not for the Fangar station (Table 1). A closer inspection revealed that for the Fangar station only scenes with 1, 2 or 3 good pixels per scene were available, due to proximity of land and bottom reflection. Highest FU values –towards brown water- were, however, derived at station 2 in Fangar Bay (FU 16). Such high FU values (above 10) were, however, all observed in scenes with only 1 pixel available and could not be confirmed by independent match-up ground measurements.

Table 1 Minimum and maximum FU water colour values over the year 2011 at six stations in Alfacs and Fangar bays. Comparison of reflectance systems and traditional measurements at station 4 in Alfacs Bay are set in bold.

	Alfacs station (central to interior)						**Fangar station (exterior to central)**					
	1	2	3	4	5	6	1	2	3	4	5	6
Jan-Dec FU min MERIS	7	6	6	**6**	6	7	6	7	8	7	7	7
Jan-Dec FU max MERIS	9	9	9	**9**	9	9	13	16	13	13	13	13
May-July FU min platform	-	-	-	**8**	-	-	-	-	-	-	-	-
May-July FU max platform	-	-	-	**10**	-	-	-	-	-	-	-	-
May-July FU min LaMotte	7	7	7	**7**	7	7	6	7	6	8	8	7
May-July FU max LaMotte	9	9	10	**10**	10	9	8	14	9	9	8	8

Weekly in-situ measured FU colour from May to July reveal a general greening of water in both bays over time. Naturally, water at stations towards the outside Mediterranean- especially station 1 in Fangar Bay, has by trend lower -meaning more blue- FU colours. Especially in Fangar Bay, water colour changes over short distances and time scales are visible (Figure 4), with highest FU values at station 2 (see 2011-05-19, Figure 4).

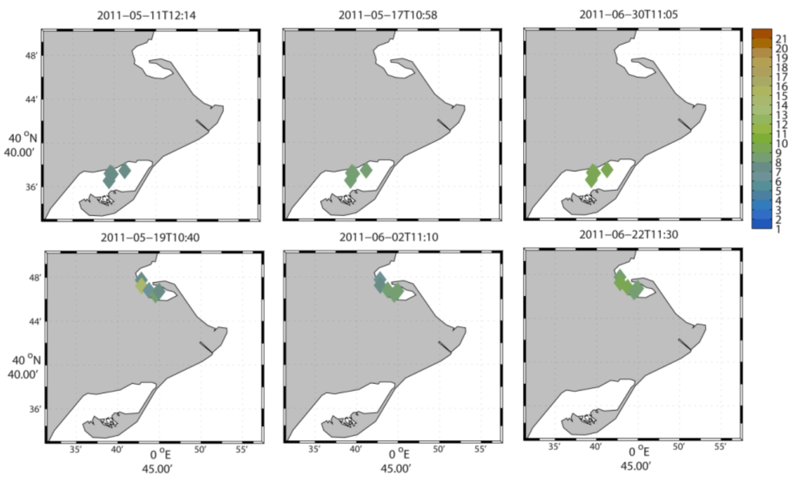

Figure 4 Variations of measured FU values at selected dates between May and July 2011 in Alfacs & Fangar bays along transects.

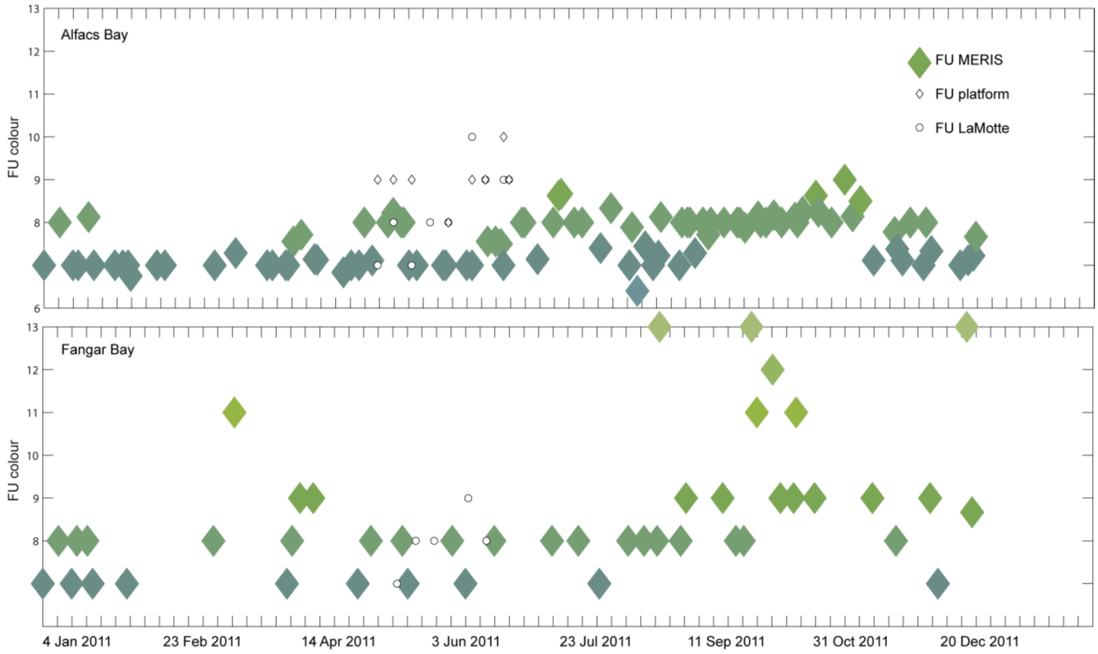

Figure 5 Temporal dynamics of water colour changes at key station 4 in Alfacs and Fangar bays in 2011. From January – December, FU as derived by conversion of MERIS reflectance data (diamonds, colour corresponds to FU colour) is plotted over time, from May – July, FU colour derived from a radiometric system on a platform (open diamonds), and as measured with LaMotte scale (open circles) are shown.

2.5 DISCUSSION

FU colour conversions of reflectance data from a radiometric system installed on a platform, as well as from MERIS are in the same ranges as FU classifications by the traditional method. Direct comparison was often impeded by lack of MERIS scenes due to cloud coverage and a relative high fraction of pixels without information. Nevertheless, it is clear that MERIS achieves a high spatial and temporal coverage. From the limited set of measurements that were obtained in the same period, there is some indication of bias between in-situ and MERIS colour. This might originate in a difference in spectral resolution between the MERIS sensor (9 bands in 300 nm) and the Ramses sensor (90 bands in 300 nm) or systematic offset in the MERIS atmospheric correction, resulting in a bluer spectrum.

The Citclops MERIS FU-colour conversion and extraction service for the Ebro Delta delivered a good overview on water colour changes over the year. It is an indication of what we might expect the Citclops App would deliver in these bays. These citizens' observations will not nicely cover a standard grid, but will be mainly positioned along the shore line. But that is exactly where the MERIS data are most corrupted and so the two sources are complementary. Also the in situ dataset of measured FU values, which represent a type of Citclops measurements by citizens, revealed more details than the MERIS data. Changes over short distances and time frames are indicative of fast dynamics of phytoplankton in the area, which were also observed over depth at the same time (*8*).

First inspection of the data indicate a higher occurrence of green water, which matches the expected seasonal pattern described by Llebot *et al*. (*6*), with higher plankton proliferations towards autumn. Different water masses were clearly distinguished by FU colours, especially at station 2 in Fangar Bay, which is close to an inflow of a freshwater canal from rice fields. Such high FU values with yellow/brown hues correspond to this source of dissolved and suspended organic material inflow to the bay.

Thereby, even such simple measurements of 21 hues of water colour aid to complete our understanding of spatio-temporal dynamics. They also complement more accurate in-situ observations that allow the identification of harmful taxa and phycotoxins. Hence, Citclops observations have a potential to support phytoplankton surveillance for human health and food safety. Both, citizen´s knowledge about the system and about effects of their measurements raise identity and awareness. This provides a strong motivation for the general public to get engaged in environmental observation and stewardship.

2.6 REFERENCES

1. J.L. Shirk, H.L. *et al*., Public Participation in Scientific Research: a Framework for Deliberate Design. *Ecology and Society* **17** (2012).
2. S. Novoa, M. R. Wernand, H. J. van der Woerd, The modern Forel-Ule scale: a 'do-it-yourself' colour comparator scale for water monitoring. *J Europ Opt Soc Rap Public* **9**:14025 (2014).
3. H. J. van der Woerd *et al*.,. Key scientific aspects of Quality Control. Public deliverable of FP7 project Citclops (2013). URL: http://citclops.eu/media/citclops/org/documents/public%20deliverables/citclops_d2.4_key_scientific_aspects_of_qc_v1.1.pdf Accessed at 2014-08-28.
4. E. Berdalet *et al*. Phytoplankton variability modulation by the hydrodynamic regime in Alfacs Bay (NW Mediterranean). A combined experimental and modelling study. In: In: H-G Kim *et al*. (eds.) *Proceedings of the 15th International Conference on Harmful Algae*, Changwon (Korea), (in press).
5. M. Delgado (1987) Fitoplankton de las bahias del delta del Ebro. *Inv Pesq* **51**:517-548.
6. C. Llebot *et al*., (2011) Hydrographical forcing and phytoplankton variability in two semi-enclosed estuarine bays. *Journal of Marine Systems* **86**:69-86.
7. M. Fernández-Tejedor, M. A. Soubrier-Pedreño, M. D. Furones, Acute LD50 of a *Gyrodinium corsicum* natural population for *Sparus aurata* and *Dicentrarchus labrax*. *Harmful Algae* **3**:1-9 (2004).
8. J. A. Busch, Phytoplankton dynamics and bio-optical variables associated with harmful algal blooms in aquaculture zones. PhD thesis at Universität Bremen (2013).

9. J. A. Busch, J. D. Hedley, O. Zielinski, Correction of hyperspectral reflectance measurements for surface objects and direct sun reflection on surface waters. *International Journal of Remote Sensing* **34**:6651-6667 (2013).

10. M. R. Wernand, A. Hommersom, H. J. van der Woerd. MERIS-based ocean colour classification with the discrete Forel–Ule scale. *Ocean Sci* **9**:477-487 (2013).

3 The plastic scale and congruence with App data

3.1 Introduction

Framed within the European Project CITCLOPS (Citizens' Observatory for Coast and Ocean Optical Monitoring), the aim of this study is to present a number of tools that can be employed by citizens to estimate the color of natural waters. Firstly, a scale that accurately matches the original Forel-Ule (FU) colors was developed using accessible and affordable materials. This Modern FU scale is presented as a 'Do-It-Yourself' kit that can be prepared using high-quality illumination filters and a frame made of a white Plexiglas (or other white material). Secondly, a smartphone application (APP) prototype that could be used by anyone willing to participate in environmental monitoring is presented. This application includes a digitalized color-comparator scale, simulating the colors of the original Forel-Ule scale, to be compared to the color of water bodies, and allows the observer to take a picture of the water body to calculate the FU number using a specific algorithm. It also offers an option to include a Secchi disk depth estimate and the Forel-Ule number obtained with the Modern FU scale, if the observer is in possession of these tools. The first inputs provided by selected volunteers and researchers, offer initial comparisons between the two monitoring tools, the Modern FU scale and the digital scale included in the smartphone application. The idea is to provide a water quality index appropriate for participatory science that allows for rapid estimates and interpretation of color changes occurring in the aquatic environment, and that could be used by local or global authorities as an assessing tool.

3.2 Background

The color of natural waters has been measured globally and intensively by oceanographers and limnologists since the 19th century by means of the Forel-Ule (FU) color comparator scale (1–3), resulting in one of the longest oceanographic data series after the Secchi disk depth. Wernand et al. (4) used these data sets to estimate global changes occurring in the ocean in relation to the chlorophyll-a concentration, a key index of phytoplankton biomass and primary productivity studies (5). It was also shown that the FU scale is related to colored dissolved organic matter (CDOM) absorbance, considered as well to be one of the water quality indicators (6). In coastal and continental areas, the color of natural waters not only strongly affects the visual and aesthetic perception of the public and their recreational use (7, 8), but has also a strong effect on aquatic ecosystems, as it has been shown to affect photosynthesis and primary productivity (9), predation regimes of herbivores (10), invertebrate behaviour (11, 12) and alter the availability and toxicity of heavy metals to fish (13, 14). Changes in color and clarity in aquatic systems can be caused by natural phenomena, but can also be due to anthropogenic activities. Therefore, to determine if a change in color is caused by a particular anthropogenic activity, it is important to collect long-term data on the color and clarity of water bodies, making it necessary to have fast and affordable tools to cover large areas, as well as a high sampling frequency. Participatory science can be a valuable method to obtain a large amount of data extended over large areas, but it requires providing citizens with user-friendly monitoring tools. Clarity of natural bodies can be easily and affordably estimated by means of a Secchi disk (20, 21). Color, is a more difficult feature to measure as it requires the analysis of the wavelength distribution of light, which can be achieved using a spectroradiometer. However, this type of instrument is expensive and not suitable for citizen monitoring surveys nor fast interpretation. The FU scale is a simple tool that can be easily used to assess the color of water bodies by citizens. The original FU color comparator consists of 21 colored solutions, ranging between indigo blue and cola brown, going through green. These solutions, made with distilled water, ammonia, copper sulfate, potassium-chromate and cobalt-sulfate, are contained in vials. The color is determined by comparison of the color of the water observed above a Secchi disk, at half its depth, to the colored vials. Although easy to use, this scale is not simply reproduced (22) and the chemicals used to prepare the solutions can be toxic to humans (23). Therefore, the idea of reproducing a more user-friendly scale arose. Interestingly, Davies-Colley (15, 16) showed that a colour-matching method using the Munsell system (17, 18), one of the most widely known colour systems, is suitable for routine water resources surveys and monitoring, since humans can easily match colours observed simultaneously. This method was implemented by the National Institute of Water and Atmospheric Research (NIWA) as part of the water quality monitoring programs (19).

3.3 Approach

The first aim of this study was to develop an affordable, 'Do-it-Yourself' color scale that matched the colors of the original Forel-Ule scale, to be used in water quality monitoring programs by citizens. This scale can be manufactured with high-quality lighting filters (LEE and Roscolux) and a white frame. To select the matching color-effect filters, both visual and instrumental comparisons were carried out between several filter combinations and the colored liquids in vials, under a diffused artificial D65 daylight simulator, in a color assessment cabinet (VeriVide) with a grey coating inside. The D65 light source has a correlated color temperature of 6500 K and was selected because it represents the average daylight, at various times throughout the day and throughout the year. The color-matching procedure was conducted following the recommendations of the American Society for Testing and Materials Standard International, commonly used in the industry to assess the color differences between objects. The liquid vial and the corresponding combination of color-effect filters were placed at the bottom part of the lighting cabinet, lying flat over a white plate. Both the visual and instrumental comparisons were carried out at a 45° degree angle, labelled as 45^0 /normal geometry by the CIE and the lamp was placed above the objects at a distance of 50 cm. The visual comparison was conducted by observing simultaneously both the vials and the filters, placed side by side, 4.0 cm apart. The instrumental measurement was conducted using a Photoresearch PR-655 spectroradiometer. A detailed explanation of methods used to develop this scale and the results obtained can be found in Novoa et al. (24). The color of any object can be specified in terms of hue, saturation and brightness. Hue refers to how the color is described (e.g. 'blue' or 'green'), and it is determined by the dominant wavelength in the visible spectrum. Saturation or color purity (less saturated is more greyish than saturated, which has a more intense color) depends on the spread of energy around the dominant wavelength (25). Brightness refers to the amount of energy detected by the human eye, which is most sensitive around the green wavelength (555 nm). The differences between the colors of the vials and of the filter combinations were assessed by calculating the differences in dominant wavelength and saturation.

A first prototype of a digital version of the Forel-Ule scale was included in a smartphone APP developed by the Citclops consortium (www.citclops.eu). The colors of this scale were derived from the transmission spectra measured of the original FU scale solutions using a TriOS VIS-Spec Analyzer (22). The transmission spectra were converted to colorimetric XYZ tristimulus values (22), which were then converted to the standard RGB (sRGB) format, the most common format used by digital devices (smartphones, digital cameras, and computers), using formulae that can be found in the literature (25, 26).

The digital images acquired by the user, are sent to the Citclops data base and used to calculate the FU number by means of a specific algorithm that converts the sRGB values extracted from the digital images, to the XYZ CIE system using the conversion matrices found in Pascale (2013):

$$[M] = \begin{bmatrix} 0.4124 & 0.3575 & 0.1804 \\ 0.2126 & 0.7151 & 0.0721 \\ 0.0193 & 0.1191 & 0.9503 \end{bmatrix} \qquad \begin{bmatrix} X \\ Y \\ Z \end{bmatrix} = [M] \begin{bmatrix} \mathrm{R} \\ \mathrm{G} \\ \mathrm{B} \end{bmatrix}$$

A programming routine does a chromatic adaptation and converts the obtained XYZ tristimulus values to chromaticity coordinates, which are then used to calculate the angle (in radians) between the vector to the chromaticity coordinates of the image and the positive x-axis. This angle is then compared to the angles of the FU solutions calculated from the transmission spectra and published in Novoa et al. (22), and the corresponding FU number is assigned. This methodology is explained in Wernand et al (2013) (4).

Finally, the comparisons of FU estimates provided by observers using the Modern FU scale and the digital scale on the APP, as well as some examples of images sent by the citizens are presented.

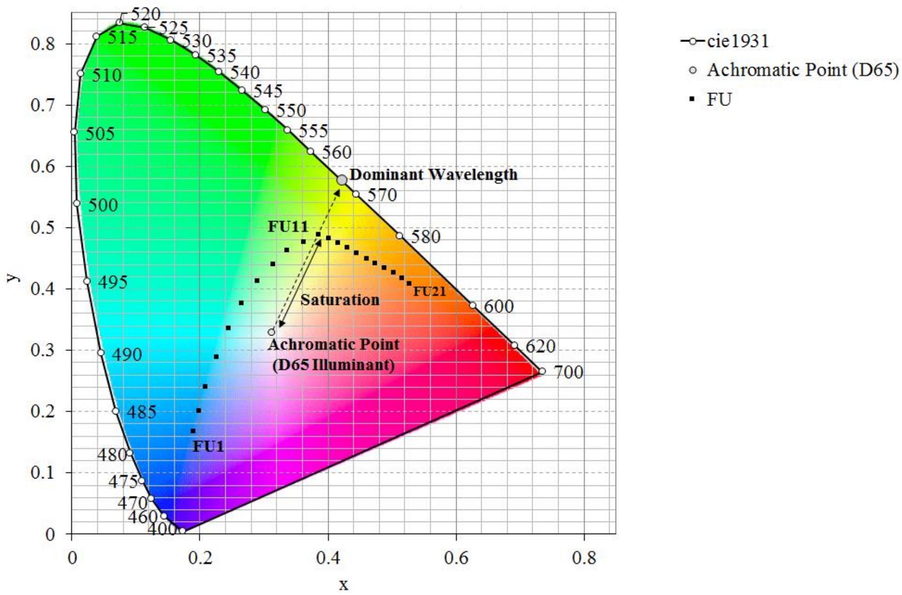

Figure 6 The CIE1931 chromaticity coordinates, based upon transmission measurements, of the FU-scale colours 1 to 21 (Novoa et al. 2013 (22)) including the achromatic point of a D65 illuminant. The outer curved boundary is the spectral locus, with wavelengths shown in nanometers.

3.4 Results

The resulting Modern FU scale is shown in Figure 7a). The format can be different, but it is important that the frame is around an A4 size and that the filters are cut with a rectangular shape of dimensions 85 x 10 mm. There should be a distance between the filters and the white background of 4 mm. A total of 30 color effect filters (27 LEE and 3 Roscolux) were necessary to match the colors of all 21 vials. The colors measured (Dominant Wavelength, DW and saturation, S) of the filters deviated a maximum of 20.83 % and 12.18 %, respectively, from the colors of the vials. Figure 5 shows the comparison of the dominant wavelength and saturation estimated for the FU vials and filters. There is a strong match in DW and S between the vials and the filters, so the selected filters were considered to be appropriate for the scale. This scale should be used to estimate the color of the water together with a Secchi disk in the same way as the original scale developed by Forel and Ule is used.

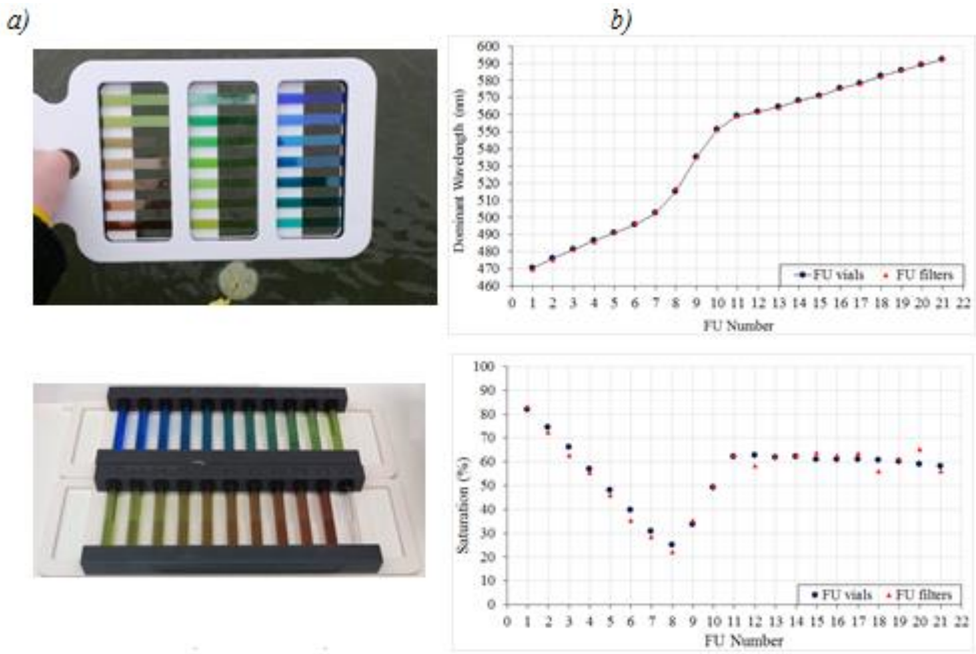

Figure 7 a) Picture of the resulting Modern FU scale, made of lighting filters, and the original FU liquid scale (bottom right). b) Dominant wavelength and Saturation percentage, respectively, of the instrumentally measured vials and filter combinations.

Twenty-one colored bars formed the digital color scale that was implemented in the Citclops application, just like the original FU scale. However, each color bar was then divided in three tones to mimic how the same FU color would be observed under different sky and light conditions (See Figure 8), and facilitate the comparison to natural water bodies. This was achieved by increasing and decreasing the saturation of each FU color. This prototype is still being tested by selected groups of volunteers, and improvements are being implemented taking into account the observers' suggestions. This first prototype, requests observers to take a picture with the camera placed on top of the water with a maximum incline of 40° with respect to the water surface and the sun on their back in case of sunny weather, to avoid sung lint. Observers are then asked to select the color on the digital scale that matches best the color of the water body observed (See Figure 7), using either the image just taken or by looking directly at the water surface. They are finally requested to answer several questions on the meteorological and location conditions.

Since the publication of the APP in April 2014, the database received approximately 150 images, where 30 of them were not pictures of the water surface, so they were removed manually. Only metadata including Modern FU estimates are compared to the FU estimates using the Digital scale. More estimates were conducted in water bodies of colors comprised between FU 9 and 14 (Figure 9), compared to the 'bluer' (FU1-FU8) or 'browner' (FU16-21) colors of the scale, so the relationship is weighted towards the first range.

Figure 8 Smartphone application for the water color comparison. The observer takes a picture following the specified protocol, compares it to the FU digital scale, and then answers questions on the meteorological and location conditions.

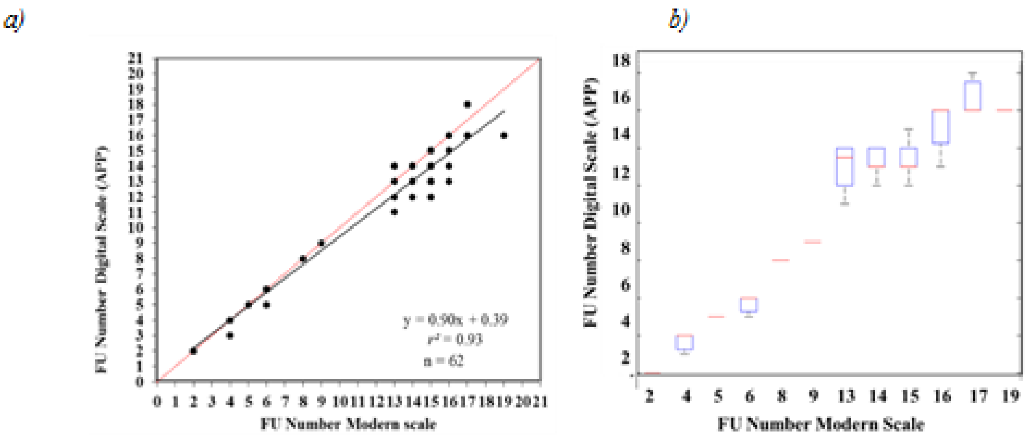

Figure 9 a) FU index estimates comparison conducted with the Digital Scale included in the APP and the FU modern Plastic Scale. b) Boxplot-whisker graph of the same comparison.

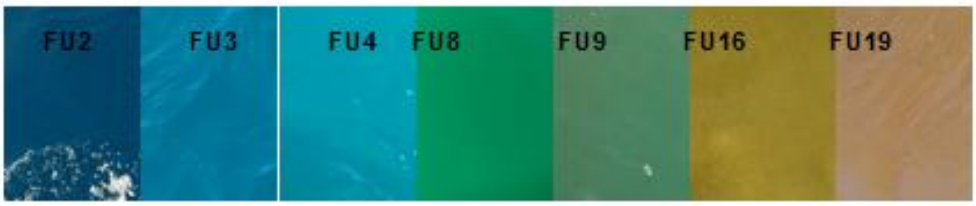

Figure 10 Example of images sent by the public, where FU index selected by the public in the digital scale matched the FU calculated by the algorithm.

3.5 Discussion and conclusions

The industrial production of standardized plastic filters has provided the means to construct a simple color comparator scale to estimate the color of natural waters to be employed in participatory science. After extensive experimentation in the laboratory, the authors are confident that the colors represented by the Modern FU scale match with appropriate accuracy the colors of the solutions of the original FU scale. The plastic filters have the advantage that the color is identical for all positions, while the thickness of the vial and the glass itself of the original FU scale, have an effect on the color perception (22). This Modern scale is an improvement with respect to the original scale, as it is light-weighted, inexpensive and easy to produce, as well as safer for the observer since there is no risk of glass breakage.

The APP will make it easier for users to estimate the color of natural waters and provide more data to the consortium, as it could be distributed easily and at no cost. Due to the different smartphone screen displays and camera characteristics, the plastic FU scale could be used as a way of validating the colors selected by the users via the application. The APP includes an option where the user can introduce the FU number measured with the Modern FU scale; the comparison of both estimates (FU from the APP, and FU from the scale) would give information on the accuracy of the digital colors. Results show a good correspondence of the water color estimated using both methods, but more comparisons are necessary. The aim is to allow observers to use the digital scale with and without a Secchi disk, for that reason different tones created by altering the saturation were introduced in each bar. Discrepancies have been observed in some cases in the selection of the FU index, with and without the disk. This occurred mostly during very cloudy and dark days, when not enough light is coming from the water column. In these circumstances, the use of the Secchi disk increases the signal coming from the water, competing like this with the sky reflection when the disk is at half its depth.

The algorithm to extract the FU from the digital images is still been optimized, so concluding results cannot be presented at this point. However, work has been carried out on images acquired by the consortium during two field campaigns, one undertaken in the North Sea and the other in coastal and continental water bodies across the Netherlands. During these two field campaigns images of the water surface were acquired, along with spectroradiometric TriOS sensors and water quality indicators, such as suspended matter, chlorophyll-a concentration and colored dissolved organic material. The results of these campaigns are very promising regarding the use of digital images to estimate the color of natural waters, based on the FU index, and will soon be published in a more detailed document. The main problem with the extraction of the FU index from images relies on the way the image is acquired by the observer and the type of camera used. Research is still ongoing on this subject, trying to find a way to minimize the users work, but also acquire all the information necessary to calculate the FU correctly.

The authors would like to emphasize that these tools are tested as part of the Citclops project, whose final objective is a proof of concept. The project needs to show that, in terms of color, an observer should be able to capture images, select the corresponding color of the water body and send the metadata collected to a database, where it is analyzed and displayed, together with additional data provided by the consortium, on an easy–to-access interface. For example, the data collected via participatory science is displayed in combination with FU layers based on satellite images (4).

To achieve this final objective, the tools that are presented here are ideal, due to their affordability and usability. In the future, the authors would like to establish more connections between the FU index and established water quality parameters. Meanwhile, the project also aims at collecting transparency and fluorescence data, which complemented with the color, will make the entire system become a remarkable water quality monitoring tool, and help raise awareness among citizens.

3.6 References

1. W. Ule, Die bestimmung der Wasserfarbe in den Seen, Kleinere Mittheilungen. *Dr. A. Petermanns Mitth. aus Justus. Perthes Geogr. Anstalt*. **38**,70-71 (1892).
2. G. E. Hutchinson, *A treatise on limnology. Vol. I, Geography, physics, and chemistry.* (John Wiley & Sons, New York, United States, 1957), p.35.
3. F. A. Forel, *Le Léman, Monographie Limnologique II.* Librairie de l'Université, Lausanne. (1982)
4. M. R. Wernand, A. Hommersom, H. J. van der Woerd, MERIS-based ocean colour classification with the discrete Forel–Ule scale. *Ocean Sci.* **9**, 477–487 (2013). DOI: 10.5194/os-9-477-2013.
5. Y. Huot *et al.*, Relationship between photosynthetic parameters and different proxies of phytoplankton biomass in the subtropical ocean *Biogeosciences*. **4**, 853–868 (2007). DOI: 10.5194/bg-4-853-2007.
6. IOCCG, in *Reports of the International Ocean Colour Coordinating Group 3*, S. Sathyendranath, Ed. (IOCCG Project Office, Darmouth, Canada, 2000), p. 144.
7. D. G. Smith, G. F. Croker, K. McFarlane, Human perception of water appearance. *New Zeal. J. Mar. Freshw. Res.* **29**, 29–43 (1995).
8. D. G. Smith, A. M. Cragg, G. F. Croker, Water clarity criteria for bathing waters based on user perception. *J. Environ. Manage.* **33**, 285–299 (1991).
9. D. L. Christensen *et al.*, Pelagic responses to changes in dissolved organic carbon following division of a seepage lake. . *Limnol. Ocean.* **41**, 553–559 (1996).
10. B. Wissel, W. J. Boeing, C. W. Ramcharan, Effects of water color on predation regimes and zooplankton assemblages in freshwater lakes. *Limnol. Oceanogr.* **48**, 1965–1976 (2003), DOI: 10.4319/lo.2003.48.5.1965.
11. L. M. Juarez, K.-H. Holtschmit, J. J. Salmeron, M. K. Smith, The effects of chemical and visual communication, space availability, and substratum color on growth of the juvenile freshwater prawn Macrobrachium rosenbergii (De Man). *J. Exp. Mar. Bio. Ecol.* **110**, 285–295 (1987).
12. A. Kullberg, Benthic macroinvertebrate community structure in 20 streams of varying pH and humic content. *Environ. Pollut.* **78**, 103–106 (1992).
13. T. A. Haines, V. T. Komov, V. E. Matey, C. H. Jagoe, Perch mercury content is related to acidity and color of 26 Russian lakes. *Wat. Air Soil Pollut.* **85**, 823–828 (1995).
14. A. Nilsson, L. Håkanson, Relationships between mercury in lake water, water colour and mercury in fish. *Hydrobiologia*. **235/236**, 675–683 (1992).
15. R. J. Davies-colley, Smith, D.G, D. J. Speed, J. W. Nagels, Matching natural water colors to Munsell standards. *J. Am. Water Resour. Assoc.* **33**, 1351–1361 (1997).
16. R. J. Davies-Colley, W. N. Vant, D. G. Smith, *Colour and Clarity of Natural waters* (Ellis Horwood Limited, Chicheste, UK, 1993), p.310.
17. Anon, *The Science of Color.* (Optical Society of America, Washington D.C., 1966), p.385.
18. A. H. Munsell, A Pigment Color System and Notation. *Am. J. Psychol.* **23**, pp. 236–244 (1912).
19. "NIWA, National Institute of Water and Atmospheric Research. National Institute of Water and Atmospheric Research. Technical report 133" (2010), (available at

www.niwa.co.nz/sites/default/files/import/attachments/Suitability-of-NZ-rivers-for-contact-recreation.pdf).

20. W. Preisendorfer, Secchi disk science: Visual optics of natural waters. *Limnol. Oceanogr.* **3**, 909–926 (1986).

21. P. A. Secchi, Relazione delle esperienze fatte a bordo della pontificia pirocorvetta Imacolata Concezione per determinare la trasparenza. Ottobre 1864. Published 1865. Memoria del mare. Il Nuovo Cimento Giornale de Fisica, Chimica e Storia Naturale. Tomo XX. (1865).

22. S. Novoa, M. R. Wernand, H. J. van der Woerd, The Forel-Ule scale revisited spectrally: preparation protocol, transmission measurements and chromaticity. *J. Eur. Opt. Soc. Rapid Publ.* (2013), DOI: 10.2971/jeos.2013.13057.

23. D. Lison, M. De Boeck, V. Verougstraete, M. Kirsch-Volders, Update on the genotoxicity and carcinogenicity of cobalt compounds. *Occup. Environ. Med.* **58**, 619–25 (2001). DOI:10.1136/oem.58.10.619

24. S. Novoa, M. R. Wernand, H. J. van der Woerd, The modern Forel-Ule scale : a “ do-it-yourself ” colour comparator for water monitoring. *J. Eur. Opt. Soc. Rapid Publ.* **9**, 14025–1:10 (2014), DOI: 10.2971/jeos.2014.14025.

25. D. Pascale, “A Review of RGB Color Spaces” (Montreal (Quebec) Canada), p. 35 (available at www.babelcolor.com).

26. G. Wyszecki, W. S. Stiles, *Colour Science: Concepts and Methods, Quantitative Data and Formulae* (New York, USA, 1982), p.950.

4 Comparison of digital imaging and calibrated spectra

4.1 Abstract

This paper describes the Water Colour from Digital Images (WACODI) algorithm, which extracts the colour of natural waters from images collected by low-cost digital cameras, in the context of participatory science and water quality monitoring. Standard RGB images are converted to the CIE XYZ colour space, undergoing a gamma expansion and illumination correction that includes the specular reflection at the air-water interface. The XYZ values obtained for each pixel of the image are converted to chromaticity coordinates and chromaticity angle (α), which is a measure of colour. Based on the distributions of α in sub-sections of the image an approximation of the intrinsic colour of the water (α_w) is found.

This algorithm was applied to images acquired in 2013 during two field campaigns in Northern Europe, one in the North Sea and the other across Dutch coastal and inland waters. The intrinsic water chromaticity angles were derived from hyperspectral measurements above and below the surface, carried out simultaneously with image acquisition. When for each station a specific illumination correction was applied, based on the corresponding hyperspectral data, a good fit (r^2=0.93) was obtained between the image and the spectra chromaticity angles (slope=0.98, intercept=-0.03). When a more generic illumination correction was applied to the same images, based only on the sky conditions at the time of the image acquisition (either overcast or sunny), a slightly *inferior*, but still satisfactory fit resulted.

This WACODI algorithm will be applied to images collected by the public via smartphone applications or 'APPs' developed within the European FP7 Citclops project. These APPs provide the option to include additional information on the water body as photographed by the user (i.e. sky conditions and viewing angle), which is important to improve the accurately of the colour retrieval.

4.2 Introduction

One commonly adopted scientific approach to assess the environmental status of water bodies is by measuring their optical properties. Together with water clarity, the colour of natural waters is the most apparent optical property of natural water. Changes in these optical properties in aquatic systems can be due to natural causes, such as plankton blooms, river outflows (transport of organic materials, nutrients and minerals), and changing meteorological conditions or can be linked to anthropogenic activities such as the introduction of an excess of nutrients originating from fertilisers used in agriculture. All these inputs will have effect on the aquatic environment. For instance, they can cause algal proliferations that affect the colour and clarity of the water, a phenomenon known as eutrophication, which is a major environmental issue across Europe (Bøgestrand et al., 2005; Ferreira et al., 2011). To determine if a change in colour is due to a particular anthropogenic activity, it is important to collect long-term data on the colour and clarity of water bodies (British Columbia Ministry of Environment 1999). To facilitate this goal it is necessary to develop citizen engaging tools to obtain high sampling frequencies and to cover large areas.

The intrinsic colour of natural waters is determined by the presence of coloured dissolved organic matter (CDOM), sediment load (Total suspended material, TSM) and gross biological activity (estimated generally through the chlorophyll-a concentration, Chl-a), which are important water quality indicators (IOCCG 2000, 2008). These components are commonly monitored for the larger areas by means of optical satellite remote sensing of the ocean (oceancolour.gsfc.nasa.gov), coastal areas (www.coastcolour.org) and even lakes (http://www.globolakes.ac.uk), since they affect water transparency, a parameter that needs to be monitored in coastal areas to comply with the European water directives (2006/7/EC; 2008/56/EC; 2000/60/EC). However, even if the satellite spatial resolution is improving and it is suitable for the open ocean, it is less accurate in coastal and inland waters (Blondeau-Patissier et al., 2004; Gohin et al., 2005). Relatively complex radiometers, airborne or at ground level, are used to improve the resolution and are used to validate satellite images. (Kallio et al., 2001; Deschamps et al., 2004; Nechad et al., 2010). However, these actions are expensive and laborious.

Wernand et al. (2013) developed a specific MERIS algorithm (named FUME), to determine the colour of natural water, based on chromaticity angles converted to the Forel-Ule index (Forel; Ule 1892; Wernand and Woerd 2010; Novoa et al. 2013; Wernand et al. 2013b). The application of this algorithm to satellite images allows classifying oceans based on their colour. In this study, the FUME algorithm was adapted to acquire RGB images using low-cost digital CCD (charge-coupled device) cameras. Colour estimation from digital images combined with participatory science could simply help fulfil the gap left by satellites monitoring water-land boundaries.

The objective of this document is to present an algorithm able to extract the colour from images of the water body based on the original FUME algorithm, with additional necessary procedures (i.e. illumination correction, gamma expansion and sub-image selection) and recommendations. This algorithm is assessed on digital images acquired during two field campaigns; one was undertaken in the North Sea and the other in coastal waters, lakes and rivers across the Netherlands. The proposed algorithm will be able to estimate the colour of natural waters from images acquired by the public, i.e. citizens using smart phones or low-cost digital cameras. Data collection is part of the EC-funded CITLOPS project (Citizens' Observatory for Coast and Ocean Optical Monitoring; www.citclops.eu).

4.3 Field campaigns

A total of 43 sampling stations were visited during two field campaigns; one in the North Sea (n=27) in March 2013, for 11 days, and the other, a 5 days campaign covering Dutch coastal and continental water bodies in August 2013 (n=16). The North Sea campaign was carried out along the East Anglia plume, where the water type is considered to be coastal due to the high suspended material concentrations generally present in the area (McManus and Prandle 1997; Dyer and Moffat 1998; Eleveld et al. 2008). The stations across the Netherlands were located in coastal areas, rivers and lakes (Figure 11) with varying composition resulting in green to dark brown coloured waters.

Water samples were collected to determine concentrations of chlorophyll-*a* (Chl-*a*) and total suspended material (TSM) and the light absorption by coloured dissolved organic material (CDOM), following the protocols for the determination of inherent optical properties of natural waters (Tilstone et al., 2002). Water samples were collected at

0.5m depth and directly filtered with GF/F filters. The Chl-*a* extraction and analysis was achieved by HPLC for the North Sea stations following the protocols developed by Jeffrey and Vesk (1997). For the Dutch inland and coastal stations Chl-*a* was estimated using spectrophotometry, following EPA's protocols (Arar, 1997). The TSM concentration was determined by the gravimetric method following the protocols established by Tilstone et al. (2002) and Van der Linden (1998). Water samples were collected, filtered with pre-weighed and pre-ashed GF/F filters (0.7 µm), and rinsed with milli-Q water. After the field work, the filters were dried and weighed for determination of TSM dry weight. For CDOM determination the GF/F filtrate of each station was again filtered over filters with 0.2 µm average pore size. Light attenuation of the filtrate in a 5 cm cuvette was analysed with a TriOS Vis-Spec analyser (320-950 nm).

At each station hyperspectral measurements were carried out using TriOS-RAMSES radiometers following the NASA protocols (Mueller et al., 2003). The measurements included sky radiance (L_{sky}), upwelling radiance (L_{sfc}) and downwelling irradiance (E_d). For calm inland waters an additional radiance measurement was carried out just below (5 to 10 cm) the water surface. The radiometers cover the spectral range 320–950 nm with a spectral resolution of 3.3nm and an accuracy of 0.3 nm. Multiple spectral measurements were carried out at each station and averaged per station. Radiance measurements were collected at an azimuth angle of 135° away from the Sun. Sky and surface radiance were measured at 35° off zenith and nadir respectively, as recommended by Mobley (1999) and Mueller et al. (2003). The radiance measurements have a viewing angle of 7°.

During both campaigns, the Samsung EK-GC100 GALAXY Camera was used to take photographs of the waters under investigation. The camera looked to the water surface in the same direction as the spectrometers at an angle between 0 and 40^0 and at approximately 135 degrees angles away from the sun to avoid sun glint, following NASA's recommendations for radiometric field measurements (Mueller et al., 2003). The Galaxy camera provides images in JPEG format.

Illumination conditions varied considerably during both campaigns due to the time of observation, the local weather conditions and water surface roughness. The cloud cover varied from overcast, to partial cloud cover, to sunny skies. Considerable differences in wind strength were found during the North Sea campaign from 1 to 25 $m.s^{-1}$. Only the sea stations sampled during calm wind and sea conditions are included in this analysis.

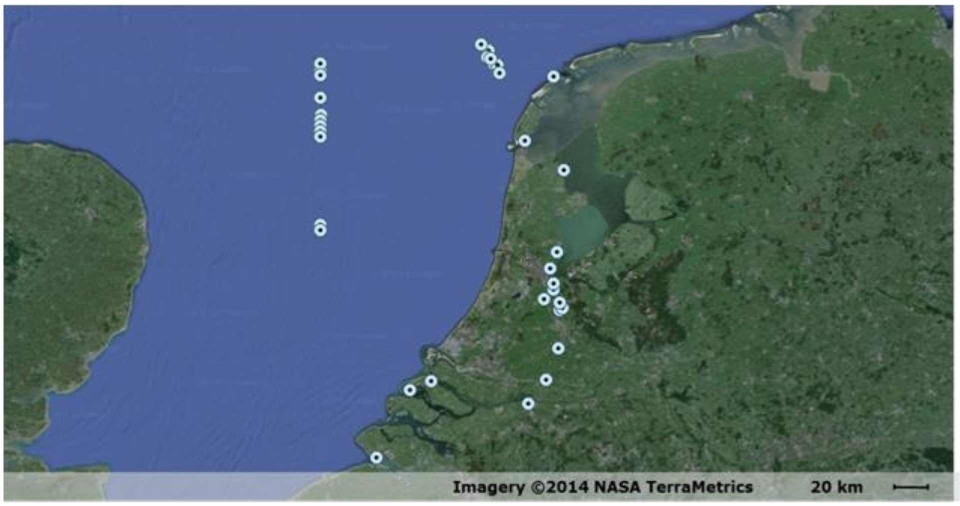

Figure 11 Map showing the location of the sampling stations in the North Sea and across The Netherlands.

4.4 Digital imaging

It has been shown that digital cameras that provide the image in raw format can basically be used as three-band radiometers (Red, Green and Blue, RGB) for water measurements, providing images with pixel values in RGB between 0 and 255 (Goddijn and White, 2006; Goddijn-Murphy et al., 2009). Raw image formats are intended to capture as closely as possible the radiometric characteristics of the scene, that is, physical information about the light intensity and colour of the scene. The three RGB values can be combined to a set of 2563 distinct colours. The majority of digital cameras in smartphones deliver images that appear very realistic to the human eye. Nevertheless, these images must be processed first before a reliable indication of the intrinsic water colour can be derived, because they are pre-processed from the raw image. Therefore, the analysis must work back from the processed images by applying a number of corrections. In this study the camera provides a widely adopted standard format: the standard RGB colour space (referred as sRGB), with a gamut (range of colours) considerably smaller than the human eye vision (Reinhard et al., 2007). The most important corrections for the sRGB format are the 'Gamma' and 'Illumination' corrections that are described in more detail below. In this paper we follow the conventions as laid out by the International Color Consortium (ICC, 2014) that has defined an open source colour management system that allows smooth communication on colour transformations between photography, printing and painting.

The illumination of water, just above the air-water interface, is determined by direct visual solar radiation and its reflection from all directions. Multiple components can contribute, like the sun, sky, clouds, rain and surrounding features like trees and mountains. But also other local effects may play a role, like the reflection at the hull of nearby boats or shadowing by ramps and jetties. All these components together define the radiation field that illuminates the water. In general, surrounding illumination is wavelength dependent and will influence the colour emerging from the water column. It is therefore essential to select the best part of the image where a reliable estimate of (α_W) can be made.

Images acquired by digital cameras have a large field of view (e.g. The Samsung Galaxy S3 camera has 4608 x 2592 pixels that cover 60.3 by 42.3 degrees). Because of this, some parts of the images could be influenced more by sky reflectance then other parts. An automated way of selecting the correct part of the image, the part which reveals the 'true colour of the water body' is therefore important.

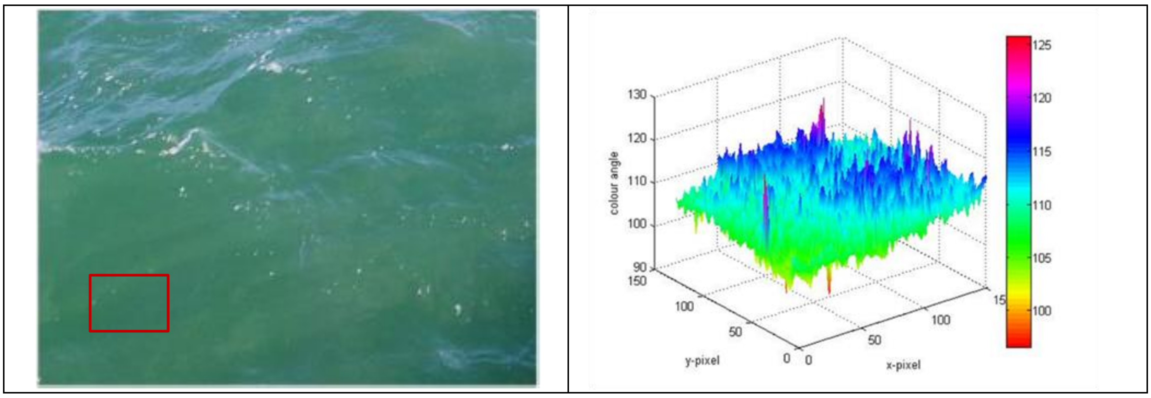

Figure 12 a) Photograph taken with a Samsung S3 smartphone from the North Sea on the 14th of March 2013. b). Graph of the chromaticity angle αW at pixel level after gamma and illumination correction of the selected sub-image (red rectangle).

However, this can also be challenging as can be seen from Figure 12a slopes that shows a typical image of the North Sea with highly variable wave slopes and white caps. Figure 12b shows the estimated (α_W) for every pixel in a small sub-section in the lower left corner (red square). The chromaticity angles (α_W) were processed according to the previously described image processing steps (eqs. 1-10).

Hence, the final step of the process is the selection of the part of the image where the colour of water can be retrieved with the least influence of surrounding colours and therefore with the highest precision. Accordingly, 8 by 6 sub-sets of with a size of 41X41 pixels are selected in each image and the distribution of the 1681 angles within each sub-pixel is analysed using percentiles (P(z)), where for example P(95) is the chromaticity angle of the 95 percentile in the distribution. For WACODI the following rules were adopted:

Natural waters all lie within specific chromaticity angle intervals. Only sub-images with that are dominated by water colours are selected; P (5) > 21 degrees and P (95) < 230 degrees. In case more information is known of the water concerned, these upper and lower limits may be adapted.

If a flat piece of water without whitecaps and relatively close to the observer is selected, the viewing and illumination geometry should be stable and all angles should fall in a narrow interval around the median. Only sub-images were selected with: P(90)-P(10) < Delta, where Delta can be chosen as a small number (here 4 degrees). To exclude artificial objects in the sub-image, a lower boundary is also adopted: P(90)-P(10) > 0.8 degrees.

When the chromaticity coordinates (x,y) are very close to the white point, the derivation with the WACODI algorithm is more sensitive to errors in the illumination correction. This effect is minimized by setting a lower limit to the distance to the white point (saturation), thereby requesting more colour expression. This was done by requiring that the median of the saturation distance has to be larger than 0.02.

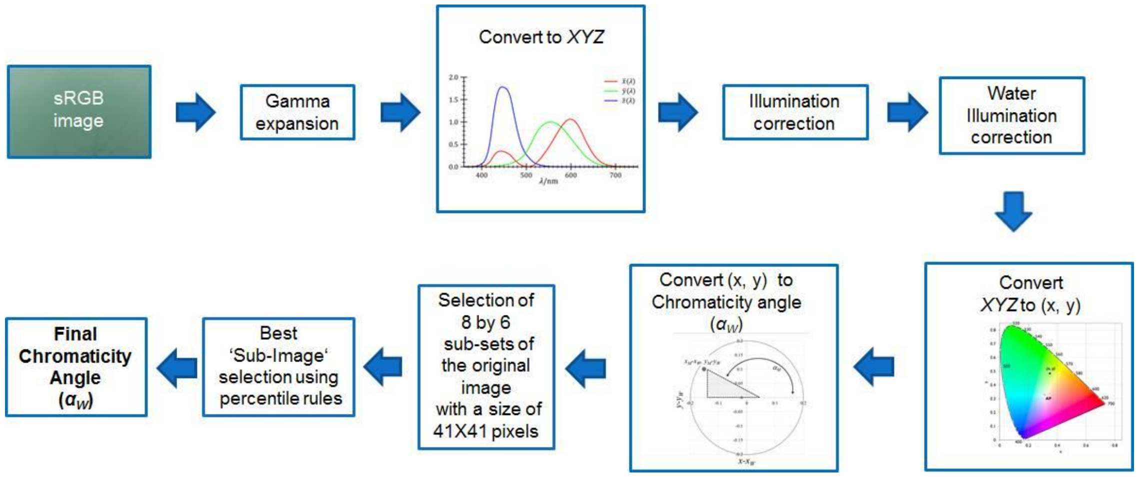

Figure 13 Summary of the algorithm procedure to extract the intrinsic colour of natural waters from sRGB images.

Finally, the minimum of the P(50) values of all sub-sections that comply with these criteria is selected. The reason is that the illumination correction is carried out for a minimum reflection at the surface (ρ = 0.029 Fresnel Reflection). Smooth water areas that are further away from the observer will have a larger ρ and therefore a larger sky contribution. In case of a blue sky, the P(50) will be bluer, corresponding with a larger colour angle.

In summary, the image is converted from *sRGB* format to the CIE *XYZ* colour space, undergoing first a Gamma expansion and an illumination correction using a correction that is specifically derived for natural waters. Following, the values for each pixel of the image are used to extract the chromaticity coordinates and finally a sub-section is selected, by means of percentiles, to derive the 'best' estimate of the intrinsic chromaticity angle of the water (α_W).

4.5 Results

The water bodies and the weather conditions covered during the two campaigns allowed for testing the WACODI algorithm for a wide range of water colours and illuminations. The concentrations of the water quality indicators varied considerably among the 43 stations, reflecting the widely different water body types that were sampled: central North Sea, coastal North Sea, rivers, lakes and even CDOM-dominated waters (peat lakes), see Table 2 for a summary

Table 2. Concentration ranges of water quality indicators (Chl-a, TSM and CDOM) and Forel-Ule index (FU) measured during the North Sea and the Netherlands campaigns.

	No. of stations	**Chl-*a* (mg.m^{-3})**	**TSM (g.m^{-3})**	**CDOM (m^{-1})**	**FU**
North Sea	27	0.54 - 3.78	0.45 - 3.06	--	6 - 13
Netherlands	16	2.36 - 55.05	1.24 - 23.94	0.47 - 3.08	9 - 19

As anticipated, the sky radiance spectra showed very different shapes for sunny conditions (very little or no clouds) compared to overcast skies, notably showing a higher peak in the blue part of the spectrum (~400 nm) in the first case. The downwelling irradiance (E_d) showed very similar shapes for both sky conditions, with a remarkable difference in magnitude (Figure 14).

Figure 14. Omitted for clarity.

From the collected E_S, L_{SKY} (shown in Figure 14) and L_{SFC} spectra the remote sensing reflectance was calculated between 400 and 800 nm according to Eq. 1 and 2. The variability in spectral shapes, due to a wide variability in the absorbing and scattering substances in the water is illustrated in Figure 15. Also the colours collected by the in-situ Forel-Ule methodology showed a large dynamic range (FU6-FU19).

Figure 15. Omitted for clarity

The R_{RS} was calculated from eq. (2), folded with the CIE1931 sensitivity curves and the colour angle (α_W) was calculated. This is referred to as the intrinsic colour or true colour of the stations. Also, E_{ill} was first calculated as a function of wavelength by eq. 10 and then converted to the *XYZ* colour vector that served as **Ws** (eq. 6 and 7). Since no digital camera observations were available that covered exactly the same spot of water and operated at exactly the same time (within 0.1 seconds from the spectrometers), a forward and inverse simulation was carried out using Matlab® software.

The L_{sfc} was first converted to an *XYZ* vector. The Y-signal (luminance) was normalized to a value between 100 and 150 to simulate the camera adaptation of the integration time to reach a DN midway between 0 and 255. The vector was converted to sRGB standards (*XYZ* to sRGB and inverse Gamma correction) and converted to 8 bits digital numbers. This vector was analysed and converted from sRGB to a colour angle of that pixel by the WACODI gamma and illumination processing software (SIM).

In Figure 16, a histogram is shown of the difference in colour angle between true and the simulation outcome (R_{RS}-SIM). The histogram shows that 68 out of 71 simulations resulted in a colour angle less than 5 degrees from the true colour. The median indicates and overall offset of minus 1.1 degrees and 76 % of the observations is found within 2 degrees from the original. The distribution is skewed and 90% of the observations (5 to 95 percentile) is found between 0.6 and -4.6 degrees.

Figure 16. Omitted for clarity

The outcome of this simulation is a proof of concept of the illumination correction along the lines of ICC (2014) written in terms of vectors and illumination correction matrices. In case this correction creates a large offset, we can quite easily identify in the original spectra the issue, such as the effects of rapidly changing condition near clouds.

The WACODI algorithm was run on the images acquired at each of the 43 stations that were visited during the North Sea and the Netherlands campaigns, using Matlab® software. The images acquired showed a wide colour range from blue-green to brown (see examples in Figure 17). In most cases only the water surface was visible on the images, but in other ones some objects appear on them.

Figure 17 A selection of images used for the determination of the intrinsic colour. Top 4 images correspond to North Sea waters. The rest of the images correspond to Dutch inland waters.

Since measurements of the radiation field above and below water were conducted, independent information was available on the intrinsic colour of the water and on the vector that should be used in the illumination correction. The regression between the α_w extracted using radiometric data and extracted from digital imaging shows a coefficient of determination of r^2=0.93 and most of the 43 images fall close to the 1:1 line as can be appreciated in Figure 18. Station 15 is represented twice, once when the part of the sub-image is selected using the minimum P(50) value and the other when the centre part of the image is selected. In the first case, there is a large offset However, when the Rrs α_w was compared to the image α_w extracted from the centre part of the image, the difference notably decreased.

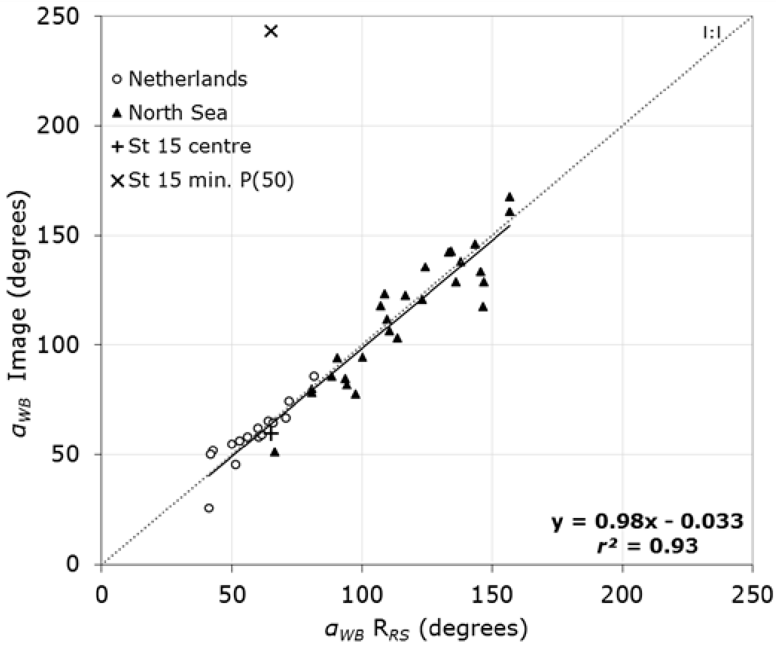

Figure 18 Correlation between chromaticity angles (αW) derived from both RRS spectra against sRGB images corrected for the illumination (section 3.3) to each station.

Subsequently, an investigation was made how WACODI performs in conditions when only the digital image is available and the detailed spectroscopic information on the illumination conditions is missing. The illumination conditions were divided into two categories: overcast and sunny. For scattered cloud conditions (CC < 4/8), the values for sunny weather conditions were assigned for that image.

The chromaticity coordinates (*x, y*) of the illumination vector **Will** extracted are shown in Figure 9 for both categories. Notice that the coordinates for sunny conditions appear far less dispersed than the coordinates for the overcast conditions. This suggests that there is an easier illumination correction for pictures acquired under clear skies, since there is a lower variability of the coordinates used for the correction. Two generic illumination vectors **Eill** were derived from the median values for either overcast or sunny weather conditions (sunny and overcast median values, Figure 19).

Figure 19 Omitted for clarity

When the same data set was analyzed with either of these two illumination corrections, the dispersion of the regression increased (r^2=0.80 vs. r^2 =0.93), while the slope of the regression line showed little variation (1.06 vs. 0.98), see Figure 10. This suggests that a standard correction could be applied to images, if the sky conditions at the time of the acquisition are known. Higher data dispersion in the higher chromaticity angle values observed (around 100 and 150) can be observed in Figure 20, which can be attributed to stations that presented scattered clouds at the time of the measurement.

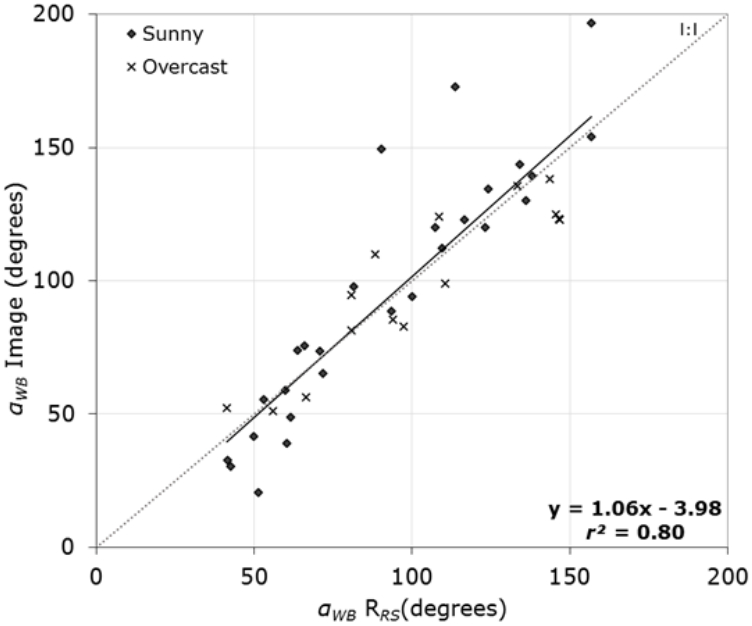

Figure 20 Correlation between chromaticity angles (αW) derived from reflectance spectra (RRS) and from sRGB images applying a two-case illumination correction; one for overcast and one for sunny/clear/scattered cloudy skies.

4.6 Discussion and Conclusions

The aquatic environment of inland and coastal waters is characterized by a complex mix of natural and anthropogenic influences and ecosystem response. In order to enhance understanding and managing practises of this dynamic environment a monitoring practise is required that provides good spatial and temporal coverage at low cost. This can be partially realized through citizens' effective participation in environmental monitoring through the use of existing devices, such as smart phones, as sensors (www.citclops.eu). In this study we have investigated if digital imagery from cameras in smart phones can be used for monitoring the intrinsic colour of natural water bodies.

The water chromaticity angle (α_W) is introduced as a simple measure to quantify the spectral distribution of the water leaving radiance. Based on extensive field work we proved that (α_W) can be extracted from sRGB digital images without bias. The extraction was done by a number of steps that included gamma expansion, chromatic adaptation and image processing. The recipe of this processing, called WACODI, is explained in detail in this paper. WACODI represents a large improvement with respect to the work conducted by Klaveness (2005), who concluded that digital cameras could only be used to document visual colour differences in a qualitative way. Our findings are in agreement with other authors (Goddijn and White, 2006; Goddijn-Murphy et al., 2009; Hoguane et al., 2012) who demonstrated that digital cameras can be used to extract quantifiable results, since they were able to correlate RGB values to the concentration of water constituents, such as chl-*a*.

During this study a number of problems were encountered that need more attention in future work. These problems cover surface roughness, illumination conditions, white balance and sub-image selection:

Surface roughness: The boundary between air and water acts as a mirror that reflects the incoming sky radiance into the camera. Although the efficiency of reflection is generally small (a few percent) it provides a large and highly variable contribution to the total measured radiance, since natural waters also have a small remote sensing reflectance value (Mobley, 1999). WACODI has included the correction for this surface reflection in the illumination correction matrix. Especially in clear sky conditions, when the illumination has a very blue characteristic colour (see Figure 14), this can have a large impact on the retrieved (α_W) when the size of this contribution is over(-under) estimated. In this respect Fig. 2b is very intriguing, showing a pixel-to-pixel variability in (α_W) that could be a combination of intrinsic variation in water composition and complex surface roughness due to capillary waves.

Illumination conditions: In the general case that an image is acquired without detailed spectrophotometric measurements, but the sky condition is known (either overcast or sunny), the estimation of water colour still can be accomplished, but with less precision. Examining the regression graph in figure 10, more dispersion can be observed in the higher chromaticity angle values (around 100 and 150) away from the 1:1 line, which can be attributed to stations that presented scattered clouds at the time of the measurement. To improve the results, the same test was achieved with 3 categories (i.e. overcast, sunny and scattered clouds), introducing the median chromaticity coordinates derived from all the stations classified as 'scattered skies', but the relationship did not improve. This was due to the high variability of illumination conditions caused by the clouds, making the median values of this category not appropriate. If cloud covers are changing fast it is more difficult to estimate the right illumination at the exact moment of image acquisition. Our recommendation to overcome this problem is to use pictures acquired under clear skies to derive an accurate chromaticity angle, because the illumination correction values are more stable for this condition.

White balance: During this study the images were acquired as close to the water as possible, to ensure correct white balancing. The white-balance setting attempts to mimic the natural colour adaptation performed by human eyes. This setting adjusts the colour of the pixels under different illuminations, using algorithms to identify the neutral tones in the photo (the whites, greys, and blacks) and then calibrate the rest of the image to the temperature of the neutral colours (Buchsbaum, 1980; Hung, 2005). This is an advantage for the user since it is easy and simple to take the picture, however it can cause problems in certain conditions, especially when objects other than the water and neutral grey/white tones are included in the picture. A widely adopted algorithm is the Grey World Assumption (Buchsbaum, 1980), which usually works reasonably well in natural scenes (Jiang et al., 2012). In this study, this setting did not present issues when the photographs were taken correctly, however, when the analysis was applied to certain images of the campaign that were taken without following the protocol precisely, the results were less successful, illustrating the importance of a correct image acquisition procedure. If future technological developments allow it, low-cost cameras will all soon incorporate several white balance and a raw format options that could be used to improve the procedure presented in this document (see also Goddijn-Murphy et al., 2009). In addition, differences in white balance procedures should be assessed among the most common smart phone and digital camera brands used in the market, to standardize the procedure.

Sub-image selection. The sub-image selection process presented here provided better results compared to other selections criteria tested, for instance selecting the centre part of the image analysed, except for one case: The station located in Markermeer De Hemmelanden, an inland marina (See the bottom right image on Figure 17). The RAMSES spectra measured at this station are very stable and similar. Two images were taken close to the jetty and gave identical results, although they were taken 30 minutes apart.

However, the situation at the jetty was very different from other stations, because the jetty was surrounded by boats and boat ramps, so probably there is a shading effect taking place on the image that was not captured by the radiometric data. Likely the sky radiation was blocked by nearby boats and did not contribute to the illumination of the water surface. Thereby, the blue light was over corrected, resulting in a bluer colour. The minimum P(50) value selected at the end of the process most likely chose the darker part on the image, but when the centre part was selected the difference between the R_{RS} derived angle α_W and the image derived angle α_W is low (α_W from R_{RS} = 65; α_W from image = 59.8). Hence, this issue indicates there should not be shades of objects present on the water surface at the moment the image is captured.

4.7 References

Arar, EJ. EPA Method 446.0 In Vitro Determination of Chlorophylls a, b, c + c and Pheopigments in Marine and Freshwater Algae by Visible Spectrophotometry, Revision 1.2 in: EPA/600/R-97/072 Methods for the Determination of Chemical Substances in Marine and Estuarine Environmental Matrices EPA US; (1997)

ASTM D1535-68. Specifying Colour by the Munsell System. Am. Soc. Test. Mater. p. 255.

ASTM E308. Standard Practice for Computing the Colours of Objects by Using the CIE System. Am. Soc. Test. Mater. p. 44.

Blondeau-Patissier D, Tilstone GH, Martinez-Vicente V, Moore GF. Comparison of bio-physical marine products from SeaWiFS, MODIS and a bio-optical model with in situ measurements from Northern European waters. J Opt A Pure Appl Opt. 2004 Sep 1;6(9):875–89.

Bøgestrand J, Kristensen P, Kronvang B. Source apportionment of nitrogen and phosphorus inputs into the aquatic environment. Report 7. Eur. Environ. Agency. European Environment Agency. ISSN 1725-9177; 2005.

British Columbia Ministry of Environment. Government, Canada. Environmental protection division. Approved Water Quality Guidelines Report . 1999. Available from: www.env.gov.bc.ca/wat/wq/BCguidelines/colour/colour_over.html, (accessed on 03/06/2014).

Buchsbaum G. A spatial processor model for object colour perception. J Franklin Inst. 1980 Jul;310(1):1–26.

Deschamps P-Y, Fougnie B, Frouin R, Lecomte P, Verwaerde C. SIMBAD: a field radiometer for satellite ocean-colour validation. Appl Opt. United States; 2004 Jul;43(20):4055–69.

Dyer KR, Moffat TJ. Fluxes of suspended matter in the East Anglian plume Southern North Sea. Cont Shelf Res. 1998;18:1311–31.

Eleveld M a., Pasterkamp R, van der Woerd HJ, Pietrzak JD. Remotely sensed seasonality in the spatial distribution of sea-surface suspended particulate matter in the southern North Sea. Estuar Coast Shelf Sci. 2008 Oct;80(1):103–13.

Fairchild MD. Colour Appearance Models. John Wiley Sons Ltd. Chichester, UK.: John Wiley & Sons, Ltd; 2005. p. 1–409.

Fairman HS, Brill MH, Hemmendinger H. How the CIE 1931 Colour-Matching Functions Were Derived from Wright – Guild Data. 1997;11–23.

Ferreira JG, Andersen JH, Borja A, Bricker SB, Camp J, Cardoso da Silva M, et al. Overview of eutrophication indicators to assess environmental status within the European Marine Strategy Framework Directive. Estuar Coast Shelf Sci 2011 Jun 93(2):117–31.

Forel FA. Le Léman, Monographie Limnologique II. Librairie de l'Université, Lausanne.; p. 651.

Goddijn LM, White M. Using a digital camera for water quality measurements in Galway Bay. Estuar Coast Shelf Sci. 2006 Feb;66(3-4):429–36.

Goddijn-Murphy L, Dailloux D, White M, Bowers D. Fundamentals of in Situ Digital Camera Methodology for Water Quality Monitoring of Coast and Ocean. Sensors. 2009 Jul;9(7):5825–43.

Gohin F, Loyer S, Lunven M, Labry C, Froidefond J, Delmas D, et al. Satellite-derived parameters for biological modelling in coastal waters: Illustration over the eastern continental shelf of the Bay of Biscay. Remote Sens Environ . 2005 Mar;95(1):29–46.

Guild J. The colourimetric properties of the spectrum. Philos Trans R Soc London Ser A, Contain Pap a Math or Phys Character. 1932;230:149–87.

Hoguane AM, Green CL, Bowers DG, Nordez S. A note on using a digital camera to measure suspended sediment load in Maputo Bay, Mozambique. Remote Sens. Lett. 2012. p. 259–66.

Hung P-C. Colour Theory and Its Application to Digital Still Cameras. Image Sensors Signal Process Digit Still Cameras . CRC Press; 2005. p. 205–21.

ICC. International Color Consortium. 2014. http://en.wikipedia.org/wiki/International_Color_Consortium

IOCCG. Remote Sensing of Ocean Colour in Coastal, and Other Optically-Complex Waters. In: Sathyendranath S, editor. Reports Int Ocean Colour Coord Gr 3. IOCCG Project Office, Darmouth, Canada; 2000. p. 144.

IOCCG. Why Ocean Colour ? The Societal Benefits of Ocean- Colour Technology Edited by : In: Platt T, Hoepffner N, Stuart V, Brown C, editors. Rep Int Ocean Colour Coord Gr 7. 2008. p. 141.

Jeffrey SW, Vesk M. Introduction to marine phytoplankton and their pigment signatures. In: Jeffrey SW, Mantoura RFC, Wright SW, editors. Phytoplankt Pigment Oceanogr Guid to Mod methods. United Nations Educational Scientific and Cultural Organization (UNESCO); 1997.

Jiang J, Zhao Y, Wang S. Colour Correction of Smartphone Photos with Prior Knowledge. Soc Photo-Optical Instrum Eng. 2012;1–6.

Kallio K, Kutser T, Hannonen T, Koponen S, Pulliainen J, Vepsäläinen J, et al. Retrieval of water quality from airborne imaging spectrometry of various lake types in different seasons. Sci Total Environ . 2001 Mar [cited 2014 Dec 2];268(1-3):59–77.

Klaveness D. Photography in limnology: documentation of lake colour using a CCD camera. Limnology . 2005 Aug 4 [cited 2013 Apr 18];6(2):131–6. Available from: http://link.springer.com/10.1007/s10201-005-0147-8

Von Kries J. Chromatic adaptation. In: Macadam D, editor. Sources Colour Sci. MIT Press. Cambridge, MA; 1970.

Lindbloom B. www.brucelindbloom.com; 2007-2010 (accessed 01/12/2014)

Van der Linde DW. Protocol for the determination of total suspended matter in oceans and coastal zones. Van der Linde, D. W. (1998). Protoc. Determ. Total suspended matter Ocean. Coast. Zo. CEC-JRC- Ispra, Tech. note no. I.98. 1998 p. 182.

McManus JP, Prandle D. Development of a model to reproduce observed suspended sediment distributions in the southern North Sea using principal component analysis and multiple linear regression. Cont Shelf Res. 1997;17(7):761–78.

Mobley CD. Estimation of the remote-sensing reflectance from above-surface measurements. Appl. Opt., 1999; 38(36): 7442-7445

Mueller JL, Fargion GS, Mcclain CR, Mueller JL, Morel A, Frouin R, et al. NASA / TM-2003- Ocean Optics Protocols For Satellite Ocean Colour Sensor Validation, Revision 4 , Volume III : Radiometric Measurements and Data Analysis Protocols. ReVision. 2003.

Munsell AH. A Pigment Colour System and Notation. Am J Psychol . University of Illinois Press; 1912;23(2):pp. 236–44.

Nechad B, Ruddick KG, Park Y. Calibration and validation of a generic multisensor algorithm for mapping of total suspended matter in turbid waters. Remote Sens Environ. 2010 Apr;114(4):854–66.

Novoa S, Wernand MR, van der Woerd HJ. The Forel-Ule scale revisited spectrally: preparation protocol, transmission measurements and chromaticity. J Eur Opt Soc Rapid Publ. 2013;

Pascale D. A Review of RGB Colour Spaces. BabelColour. Montreal (Quebec) Canada; 2003 p. 35.

Reinhard E, Arif Khan E, Ouz Akyuz A, Johnson GM. Colour Imaging: Fundamentals and Applications. 2007. p. 1058.

Thomas S, Guild J. The C.I.E. colourimetric standards and their use. Trans Opt Soc. 33(3):73–134.

Tilstone GH, Moore GF, Sorensen K, Doerffer R, Røttgers R, Ruddick KG, et al. Regional Validation of MERIS Chlorophyll products in North Sea REVAMP Protocols Regional Validation of MERIS Chlorophyll products in. 2002 p. 77.

Ule W. Die bestimmung der Wasserfarbe in den Seen, Kleinere Mittheilungen. Dr A Petermanns Mitth aus Justus Perthes Geogr Anstalt. 1892;38(70-71).

Wernand MR, Hommersom a., van der Woerd HJ. MERIS-based ocean colour classification with the discrete Forel–Ule scale. Ocean Sci . 2013a May 2 [cited 2014 Jan 8];9(3):477–87. Available from: http://www.ocean-sci.net/9/477/2013/

Wernand MR, Woerd HJ Van Der. Spectral analysis of the Forel-Ule ocean colour comparator scale. J Eur Opt Soc Rapid Publ . 2010 Apr 27;5:10014s.

Wernand MR, Woerd HJ Van Der, Gieskes WWC. Trends in Ocean Colour and Chlorophyll Concentration from 1889 to 2000, Worldwide. PLoS One. 2013b;8(6).

Wright WD. A re-determination of the trichromatic coefficients of the spectral colours. Trans Opt Soc. 1928;30(4):141–64.

Wyszecki G, Stiles WS. Colour Science: Concepts and Methods, Quantitative Data and Formulae. John Wiley & Sons, editor. New York (USA); 1982. p. 950.

5 The light attenuation measurements

5.1 Abstract

The low cost moored system KdUINO allows to measure parameters related to water transparency, specifically the diffuse attenuation coefficient parameter. In this contribution, its measurements are compared with other high precision scientific commercial instrument in order to estimate the sensor measurement error.

5.2 Introduction

A widely adopted, scientific approach to assess the environmental status of water bodies is by measuring their properties, such as color, fluorescence, and transparency. The transparency of natural water is affected by the presence of dissolved organic matter, sediment load and phytoplankton, which are considered water quality indicators.

There are different ways to measure water transparency: from the simplest Secchi disk, dating back to the XIX century, which is a white disk held by a rope that is lowered into the water until it is impossible to see it, to the most advanced oceanographic radiometers. However, all these instruments only allow getting punctual data as the Secchi disk has to be dipped by hand each time a data is needed and the other instruments are expensive and costly to use as well as always connected to a power station.

Citizen science projects take advantage of low-cost technologies and citizen collaboration to get big amount of data. One of the most famous one is the Secchi Dip-In [1], where Secchi disks are used to measure water transparency. It demonstrates the great potential of citizen volunteer based collected data in order to obtain important information on lakes, rivers and ponds. Other projects of citizen participation such as Citclops [2], exploit the available technological facilities (such as mobile phones and embedded technology) to measure easily and accurately parameters related to the optical properties of the water (color, fluorescence, and transparency).

The great technological advances in embedded systems and sensors have increased people's interest in creating their own instrumentation equipment. Moreover, these new developers share the collected data with the scientific community by using existing communication infrastructures (web pages and social networks). With these ideas in mind, in the context of the FP7 project Citclops, we designed the KdUINO (see Figure 21), a moored system with low-cost sensors, based on the open hardware platform Arduino [3] and quasi-digital sensors that measure parameters related to the water transparency at different depths. A detailed description of the system components can be found in [4] from the same authors where the same buoy was named cBuoy. The KdUINO has been designed as a DIY (Do-It-Yourself) instrument: it is very easy to build and to use even for laypeople and can be made at home. Its total cost is of less than 200 Euros. This type of instruments increments the marine citizen science community and crowdsourcing capabilities, allowing a much larger spatial and temporal monitoring of parameters related to water quality. The objective is to provide the resulting processed data to the public, the scientific community and decision-makers. Another advantage of such project is that involving laypeople increases their awareness of the importance of water quality and of scientific research.

Figure 21 KdUINO, a "homemade" buoy used to calculate the diffuse attenuation coefficient of the water.

The KdUINO sensors measure light irradiance (the power of electromagnetic light radiation per unit area incident on a surface) at different depth from which we can calculate the diffuse attenuation coefficient parameter (*K*). *K* characterizes how easily a material or medium can be penetrated by a beam of light, sound, particles, or other energy or matter. A large attenuation coefficient means that the beam is quickly "attenuated" (weakened) as it passes through the medium, and a small attenuation coefficient means that the medium is relatively transparent to the beam. For this reason, attenuation coefficient is well related to transparency [5]. In the case of the water, K_d is the diffuse attenuation for downwelling irradiance and K_u is the diffuse attenuation coefficient for upwelling irradiance. Depending on the type of irradiance measurement sensor and its capsule, it can measure planar irradiance, scalar irradiance or specific angle irradiance. Scalar irradiance is defined as the irradiance from all directions (360º) equally weighted and planar irradiance as the irradiance from 180^o.

In this contribution, the measurements and results of the KdUINO are analyzed and compared to ones obtained with an oceanographic radiometer in order to validate them. This work will also demonstrate that with a post-processing analysis of the measurement data of the KdUINO, it is possible to obtain a parameter whose value is very close to the K_d obtained with expensive high precision radiometers.

5.3 Instruments and measurements used in this study

The KdUINO contains an Arduino platform working as a control unit located in the plastic container (see drawing in Figure 22) and several quasi-digital optical sensors placed at different depths. The sensors [6] convert the irradiance measurements into frequency. The system simply counts the number of cycles over large periods of time (several minutes) to obtain a time integrated measurement of irradiance values near the water surface. The integration is equivalent to an averaging and reduces the measurement variability derived from the large light fluctuations caused for example by focusing of sunlight by surface waves [7].

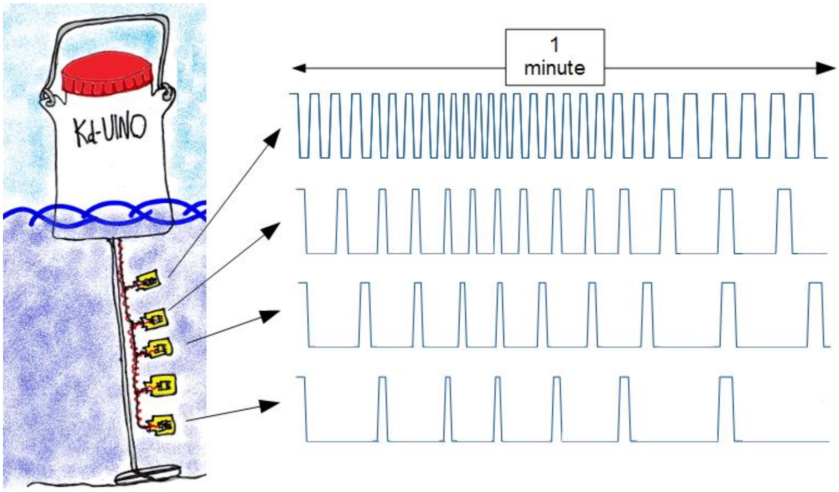

Figure 22 Graphical example of how KdUINO estimates an average value of a fluctuating underwater light.

Beer-Lambert's law applied to liquid medium, states that light intensity decreases exponentially as a function of depth in the water column and is described mathematically in (1).

$$E = E_0 e^{-Kz} \quad (1)$$

or

$$\ln(E) = -Kz + \ln(E_0) \quad (2)$$

Where E is the irradiance of the light at given depth, E_0 is the irradiance of the light at the surface, K is the attenuation coefficient and z is the depth. The KdUINO sensor set allows to measure simultaneously light irradiance E at different depths. So it can be seen from (2) that the attenuation coefficient k is simply the slope of a regression line and can be easily deduced from the measured irradiance. Figure 23 shows an example of the regression slope computed from a real experiment where each diamond corresponds to a measurement and the dotted line is the regression line.

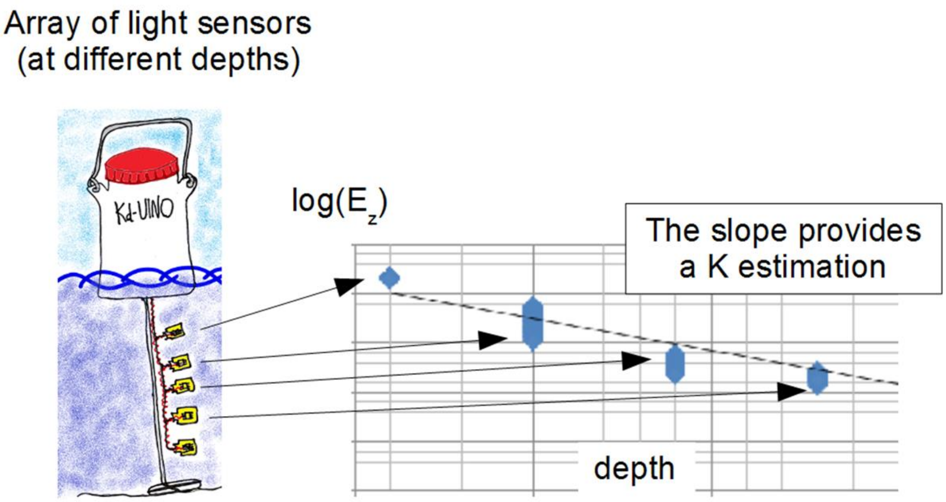

Figure 23 K parameter calculated with based on some KdUINO data.*

The KdUINO sensor measurements are subject to some unknown factors, both electronic and mechanic. For this reason and to distinguish it from the real K_d, in this study the diffuse light attenuation coefficient calculated from the KdUINO data is called *K**. The unknown factors are the following ones:

- Sensor tolerance: the technical specifications of the sensors indicate that they are available with an absolute output frequency tolerance of 20%.
- Light integration: the light integration response of the sensors depends on the form and material of the capsule's sensor. The capsules are "homemade" and the irradiance measurement can change depending on the chosen one (some design examples are shown on Figure 24).
- Changes in wavelength illumination: the technical specifications of the sensors contain imprecise information on the outcome variation as a function of wavelength. The datasheet just contains information on the output frequency (kHz) versus the irradiance (μW/cm2) at 640 nm (fig.1, page 4 in [3]). This imprecise information induces some errors in the calculation of *K**.
- Photodiode spectral responsivity: the received light irradiance varies from 300 to 1100 nm. The output frequency varies in function of the received light irradiance integrating the entire spectrum.

Even knowing that the measured parameters are not the same, measurements have been compared to check that changes in transparency detected with high precision instrument are also detected with KdUINO.

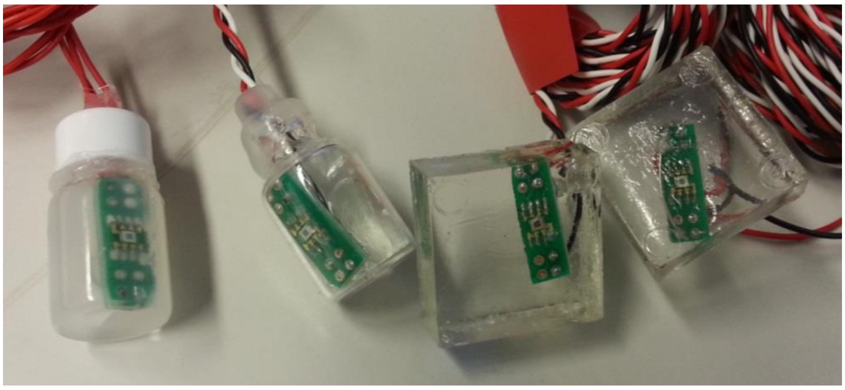

Figure 24 Sensor's capsules.

In this study, we used the PRR-800 which is a High Resolution Profiling Reflectance Radiometer [7]. The instrument combines high-resolution radiance and irradiance optics, a high-speed data acquisition system. It measures E_d (downwelling irradiance) and L_u (upwelling radiance) at 15 different wavelengths in the spectral range of 305-875 nm with a bandwidth of 10 nm. The values of E_d are going to be used in this study to obtain the K_d. As the KdUINO sensors integrate all the wavelengths, to accurate the comparison between both instruments, all the measurement wavelength values of the radiometer are going to be integrated to obtain a single value at each depth.

In contrast to KdUINO, which can measure continuously over a long period of time simultaneously at different depths, the radiometer only gets data at a punctual point of the water column. Numerous studies begin their analysis of K_d discarding the first meters of depth [8] because of large changes in light detected by [7], where the effects of light and waves are most prominent. However, the objective of the project is to study coastal waters, with only a few meters of depth. To mitigate this problem with the radiometer we averaged many measurements taken at the same depth for a few minutes, see Fig. 5. In Figure 25c, the red line represents the integrated values on all wavelengths along the depth computed from Figure 25 and the discontinuous line the regression line.

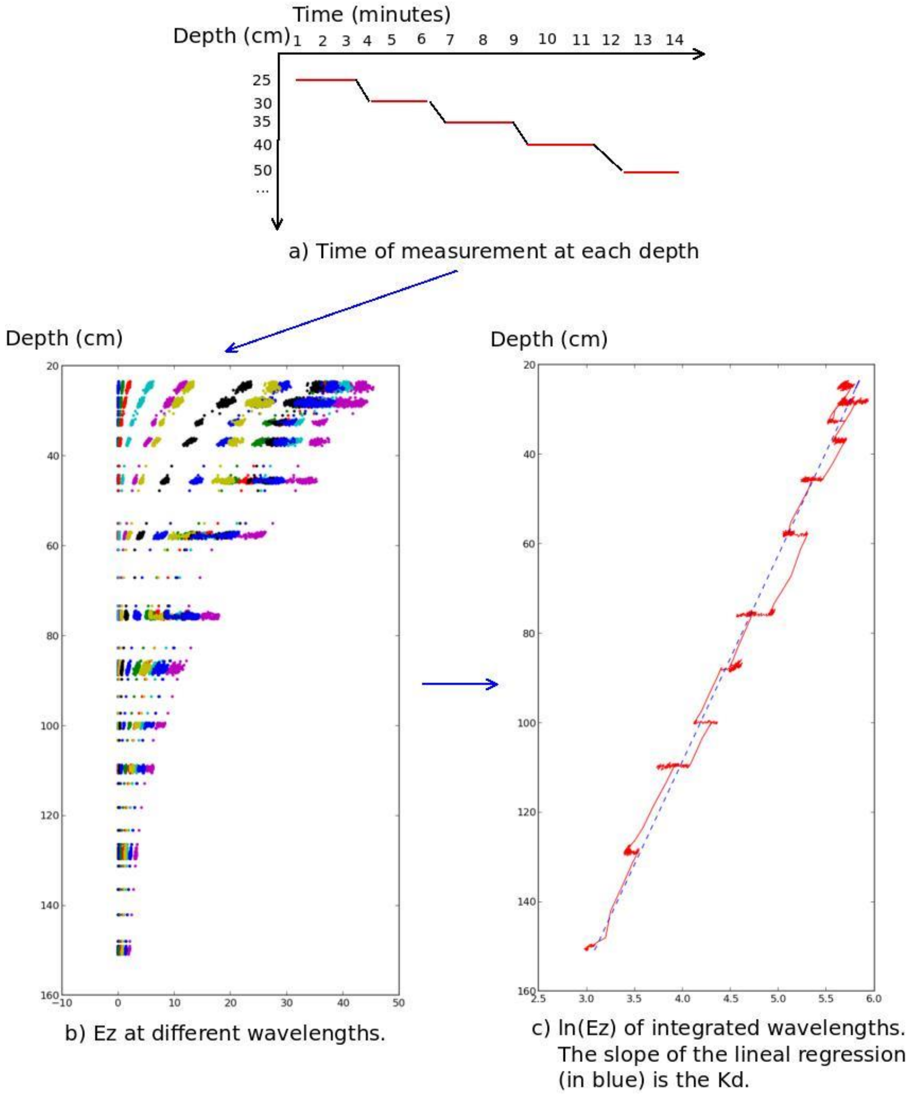

Figure 25 Radiometer measurement process.

5.4 Comparison of measurements

Before thinking on the quality of the data, we have to make sure that the system is stable that is to say, if two sets of data are collected in the same conditions (environmental conditions, physical ...) at different moments, the values should be similar.

Therefore an experiment was performed to calculate the parameter *K** from the data obtained measuring continuously during one hour with the KdUINO. The experiment was carried out on a coastal area with very few waves and a fairly clear day. The experiment being conducted in the field, not in a laboratory where everything is controlled, we cannot expect the system to measure exactly the same values but, to be valid the system, they should be similar. Figure 26 shows the result of the experiment, demonstrating that KdUINO is very stable.

In August 2013, a field campaign was conducted at the Dutch coast. One objective was to compare the values of *K** obtained with the KdUINO and of K_d obtained with the radiometer. Both instruments measured at 6 different points of the Dutch coast, where transparency and color seemed to be different. The values of *K** from the KdUINO and of K_d from the radiometer were calculated and compared. As can be seen on Figure 27, the regression coefficient of the line formed by the points is 0,95513. This indicates a strong similarity between the two sets of values. According to Table I, the measurement errors are low and comparable with many commercial measuring instruments. Measurement errors increase in very clear water, but remains within acceptable levels. The average of the measurement error is 5,10%.

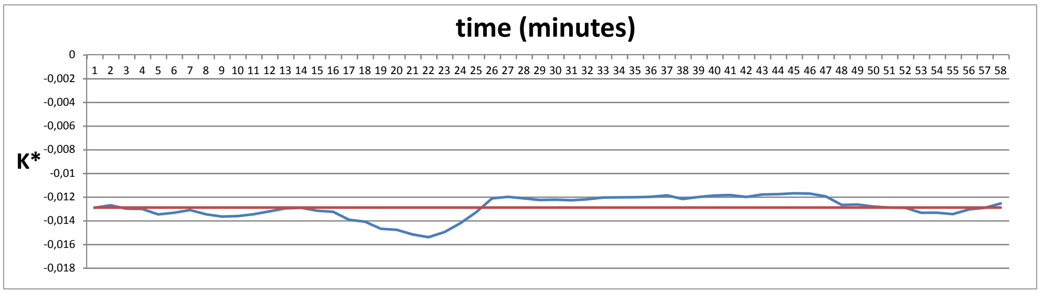

Figure 26 Results of K computed from the KdUINO measurements during 1 hour in a "stable" coastal zone.*

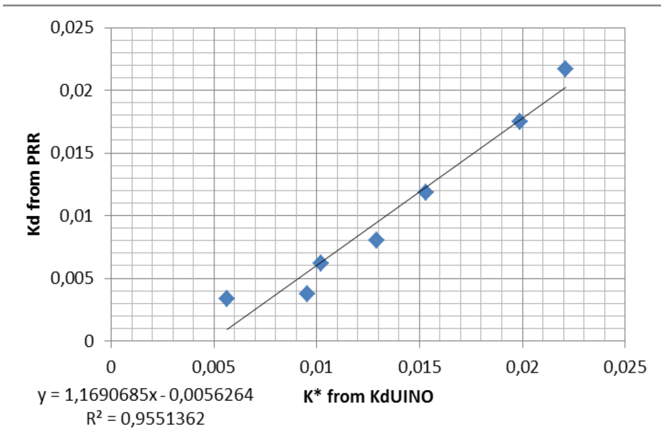

Figure 27 Comparison of K results with two different instruments. They are highly linearly correlated (r2=0,95513).

Table 3 Error of measurements with the KdUINO

K_d radiom.	***K**** **KdUINO**	***K_{d}_reconst***	**Error (difference)**	**Full scale error (max val 0.0216)**
0.0216753331	0.0221228	0,02023669	0,00143864	6,64%
0.017519585	0.0198888	0,01762499	0,00010540	0,49%
0.0118272853	0.0153246	0,01228913	0,00046184	2,13%
0.0080460267	0.0129021	0,00945706	0,00141103	6,51%
0.0061734301	0.0102	0,00629812	0,00012469	0,58%
0.0037633688	0.0095406	0,00552723	0,00176386	8,14%
0.00337504	0.0056226	0,00094682	0,00242821	11,20%

Table 3 shows the measurement error, where:

- The first column shows the K_d calculated with the radiometer data.
- The second column shows the K^* calculated with the KdUINO data.
- The third column shows the K_d constructed from the linear regression equation of Figure 27, described in (3).

$$K_d\_reconst = 1{,}1690685K^* - 0{,}0056264 \qquad (3)$$

- The fourth column shows the difference between K_d_reconst and K^* from the KdUINO.
- The fifth column shows the full scale error. The full scale error is the absolute error divided by the range, the full scale (the maximum value of K_d). The full scale error is described in (4).

$$FS\_Error = \frac{K_d - K_d\_reconst}{0{,}0261} \qquad (4)$$

To have a more precise information on the measurement error, a complementary test should be performed in a laboratory where control light and water type are exactly known. Anyway, the relative error values indicate at least that the measurement error is small and the study goes in the right direction.

5.5 Conclusion

The KdUINO is a “homemade” buoy that is able to measure a parameter related to water transparency, the diffuse attenuation coefficient. The preliminary results indicate that the KdUINO is a very stable measurement instrument. Some of the KdUINO light sensor parameters are not known. For this reason it is not possible to exactly know what type of diffuse attenuation coefficient can be calculated (K_d, K_u, scalar, planar...). Anyhow, preliminary results comparing the KdUINO results with oceanographic radiometer ones show that post-processed KdUINO measurements give a K^* parameter similar to K_d, with a relatively low error.

One of the advantages of the KdUINO is that it will allow to set a wide set of sensors measuring transparency in a permanent or semi-permanent way, with a spatio-temporal coverage unreachable with conventional instruments because of their costs and/or their lack of possibility to record data in a long term.

As stated in section III, comparison of data measurements from the KdUINO and from classical instrumentation should be performed in a controlled laboratory to get more precise ideas on the errors associated to the KdUINO.The system mechanics should be improved and other light sensors tested.

5.6 References

1. www.secchidipin.org/ [Accessed: 25 February 2014]
2. www.citclops.eu [Accesed: 25 February 2014]
3. www.arduino.cc/ [Accessed: 25 February 2014]
4. Bardaji, R and Piera J. Low-cost moored instrumentation for citizens' education and participation in environmental stewardship. OCEANS - Bergen, 2013 MTS/IEEE, Norway, 10-14 June 2013
5. *Physycs for Scientists and Engineers: Strategic Approach*. Vol. 1, Chap. 4. Content Technologies, Inc. 2013.
6. www.ams.com/eng/Products/Light-Sensors/Light-to-Frequency/TSL230RD [Accessed: 25 February 2014]
7. M. Darecki, D Stramski, M Sokólski. Journal of Geophysical Research. 116, C00H09, 2011
8. PRR-800 Profiling Reflectance Radiometer Brochure. Biospherical Instruments Inc. 2011
9. Mueller, J. L., Fargion, G. S., and McClain, C. R. “Radiometric Measurements and Data Analysis Protocols. In Ocean Optics Protocols for Satellite Ocean Color Sensor Validation”, Revision 4, Volume III, NASA/TM-2003-211621/Rev4-Vol. III, NASA Goddard Space Flight Center, Greenbelt, Maryland.

6 Summary of early findings

This is a report of the early findings, regarding the congruence between crowd-sourced, external and calibrated data. The deliverable was planned to report on the congruence of data collected with the App and the relation to existing and well known data at PM24. However, at that moment insufficient material was available to do a reliable analysis, because:

- The number of colour observations by the App in the database was limited
- The MERIS data from the CoastColour project were reprocessed (version 2) by the provider and NOVELTIS was in the process of downloading and reprocessing plus the lack of actual collected MERIS data at the Citclops project time due to decay of ENVISAT.
- The observation of light Attenuation (KdUINO) and fluorescence were not yet operational.

It was concluded by the PB that the best way forward was to focus this deliverable on material that has been collected in field campaigns and provide well calibrated data, amongst others:

- In-situ data from RAMSES spectrometers and LaMotte colour scale, collected by dr. J. Busch (Uni Oldenburg) in the Ebro Delta in 2011, in combination with reprocessed data of MERIS.
- RAMSES spectrometer data above water, RAMSES spectrometer data below water, RGB Image of the water and FU scale number derived from the plastic and fluid scale above a Secchi Disk, collected. at the campaigns on the North Sea and in The Netherlands in 2013
- Measurements of KdUINO made during the campaign in The Netherlands in 2013.

The following promising results were achieved:

Colour conversions of reflectance data from a radiometric system installed on a platform, and from the satellite-based MERIS instrument are in the same range.

Direct comparison is often impeded by lack of MERIS scenes due to cloud coverage and a relative high fraction of pixels without information.

There is some indication of bias between in-situ and MERIS colour. This might originate in a difference in spectral resolution between the MERIS sensor (9 bands in 300 nm) and the Ramses sensor (90 bands in 300 nm) or systematic offset in the MERIS atmospheric correction, resulting in a bluer spectrum. (Section 2,4; Figure 5).

Seasonal phytoplankton patterns are well reflected by MERIS FU data at core site Ebro Delta. Hence, climatology can be used as reference also for upcoming citizen data.

The industrial production of standardized plastic filters has provided the means to construct a simple colour comparator scale that matches with the colours of the solutions of the original FU scale with appropriate accuracy.

FU index estimates comparison conducted with the Digital Scale included in the APP and the FU modern Plastic Scale has been quantified (Section 3.4; Figure 9).

The intrinsic water chromaticity angles were derived from hyperspectral measurements above and below the surface, carried out simultaneously with image acquisition. When for each station a specific illumination correction was applied, based on the corresponding hyperspectral data, a good fit (r^2=0.93) was obtained between the image and the spectra chromaticity angles (slope=0.98, intercept=-0.03), see section 4.5; Figure 18.

When a more generic illumination correction was applied to the same images, based only on the sky conditions at the time of the image acquisition (either overcast or sunny), a slightly *inferior*, but still satisfactory fit resulted (Section 4.5; Figure 20).

Comparison of the KdUINO results with oceanographic radiometer ones show that post-processed KdUINO measurements give a K^* parameter similar to K_d, with a relatively low error, see section 5.4; Figure 27 and Table 3.

7 List of Key Words/Abbreviations

Chl *a*	Chlorophyll *a*
CDOM	Coloured Dissolved Organic Matter
CIE	International Commission on Illumination
DIY	Do-It-Yourself
DOW	Description of Work
FU	Forel Ule (Water colour comparator scale)
KdUINO	Low cost buoy to measure transparency parameter Kd
MERIS	Medium Resolution Imaging Spectrometer
PB	Programme Board
PM	Project Month
RAMSES	Radiation Measurement Sensor with Enhanced Spectral Resolution
RGB	Red Green Blue
TSM	Total Suspended Matter
WACODI	Water Colour from Digital Images
WP	Working Package
WQ	Water Quality parameters